

## **General Disclaimer**

### **One or more of the Following Statements may affect this Document**

- This document has been reproduced from the best copy furnished by the organizational source. It is being released in the interest of making available as much information as possible.
- This document may contain data, which exceeds the sheet parameters. It was furnished in this condition by the organizational source and is the best copy available.
- This document may contain tone-on-tone or color graphs, charts and/or pictures, which have been reproduced in black and white.
- This document is paginated as submitted by the original source.
- Portions of this document are not fully legible due to the historical nature of some of the material. However, it is the best reproduction available from the original submission.

NASA CR- 144681

**THERMAL DESIGN SUPPORT FOR THE  
EXPLORER GAMMA RAY  
EXPERIMENT TELESCOPE**

D. W. Almgren

W. D. Lee

S. Mathias

Arthur D. Little, Inc.

Cambridge, Massachusetts 02140

**JUNE 1975**

**FINAL REPORT FOR PERIOD**

**FEBRUARY - JUNE 1975**

*prepared for*

**GODDARD SPACE FLIGHT CENTER  
GREENBELT, MARYLAND 20771**

(NASA-CF-144681) THERMAL DESIGN SUPPORT FOR  
THE EXPLORER GAMMA RAY EXPERIMENT TELESCOPE  
Final Report, Feb. - Jun. 1975 (Little  
(Arthur D.), Inc.) 24 p HC \$3.50 CSCI 22E

N76-12125

Unclas  
04785

G3/19

Arthur D. Little, Inc.

1. Report No.	2. Government Accession No.	3. Recipient's Catalog No.	
4. Title and Subtitle THERMAL DESIGN SUPPORT FOR THE EXPLORER GAMMA RAY EXPERIMENT TELESCOPE		5. Report Date June 1975	
		6. Performing Organization Code	
7. Author(s) D. W. Almgren, W. D. Lee, and S. Mathias		8. Performing Organization Report No. C-75567	
9. Performing Organization Name and Address Arthur D. Little, Inc. 20 Acorn Park Cambridge, Massachusetts 02140		10. Work Unit No.	
		11. Contract or Grant No. NAS5-23206	
12. Sponsoring Agency Name and Address Goddard Space Flight Center Greenbelt, Maryland 20771 Mr. James P. Marshburn, Code 732.2		13. Type of Report and Period Covered Final Report	
		14. Sponsoring Agency Code	
15. Supplementary Notes None			
16. Abstract <p>This report documents the results of a thermal design definition study for the GSFC Explorer Gamma Ray Experiment Telescope (EGRET). A 241 node thermal computer model of EGRET was developed and used to analyze the thermal performance of the experiment for a range of orbits, payload orientations and internal power dissipations. This computer model was delivered to GSFC as part of the effort.</p> <p>The recommended thermal design utilizes a small, 1.78 square foot, radiator on the anti-sun side of the mission adaptor and circumferential heat pipes on the interior of the same adaptor to circumferentially transfer heat from the electronics compartments to the single radiator. Fifty watts of thermostatically controlled heater power is used to control temperature level to 10°C ± 20°C inside the insulated dome structure.</p>			
17. Key Words (Selected by Author(s)) EGRET, Thermal Design Thermal Design Analysis		18. Distribution Statement	
19. Security Classif. (of this report) Unclassified	20. Security Classif. (of this page) Unclassified	21. No. of Pages 24	22. Price*

## PREFACE

The objective of this report is to document the work accomplished and the results obtained under contract NAS5-23206 during the five month period ending 30 June 1975. The scope of work was to define a thermal control subsystem for the Explorer Gamma Ray Experiment Telescope (EGRET) when mounted to a Low Cost Modular Spacecraft (LCMS) and to deliver the thermal computer model, used to define the thermal design of EGRET, to GSFC.

As a result of this five month effort, a thermal control subsystem philosophy has been developed for the low powered EGRET which utilizes heat pipes in the region of the electronics compartment, coupled to a relatively small radiator on the anti-sun side of the monocoque mission adapter. Fifty watts of heater power is utilized inside the neon gas filled pressure vessel to meet temperature level and temperature gradient requirements in both the polyvinyl toluene dome and also in the high voltage stack. This design has been analyzed with computer runs which simulated four spacecraft orientations in both a maximum and minimum percent sunlight orbit for various combinations of internal power dissipation (electronics plus heaters) and the results are documented in the Results and Recommendations Section of this report.

## TABLE OF CONTENTS

	<u>Page No.</u>
I. PURPOSE	1
II. BACKGROUND	2
III. RESULTS AND RECOMMENDATIONS	6
COMPUTER MODEL RESULTS	12
IV. DESCRIPTION OF THERMAL COMPUTER MODEL	17
SPARK CHAMBER	17
HONEYCOMB PRESSURE PLATE	21
TOTAL ABSORPTION SHOWER COUNTER	21
LOWER BOX AND ELECTRONICS' COMPARTMENTS	22
APPENDIX A    NODE BAEDEKER FOR THE EGRET THERMAL COMPUTER MODEL	A-1
APPENDIX B    NUMERICAL SURFACE NAMES FOR GEOMETRIC REPRESENTATION OF EGRET	B-1
APPENDIX C    DYNATECH REPORT ON THE THERMAL CONDUCTIV- TIVITY OF A PVT PLASTIC	C-1

LIST OF TABLES

<u>Table No.</u>		<u>Page No.</u>
1	THERMAL REQUIREMENTS FOR EGRET	7
2	ORBITAL/ENVIRONMENTAL PARAMETERS AREA IN EGRET THERMAL COMPUTER MODEL STUDIES	13
3	TEMPERATURE PREDICTIONS (°C) USING EGRET THERMAL COMPUTER MODEL	16
4	THERMOPHYSICAL AND OPTICAL PROPERTIES OF MATERIALS USED IN EGRET THERMAL COMPUTER MODEL	18
5	POWER DISSIPATIONS (WATTS) FOR EGRET	24

APPENDIX TABLES

1a	NODE BAEDEKER FOR EGRET THERMAL COMPUTER MODEL	A-2
----	---	-----

LIST OF FIGURES

<u>Figure No.</u>		<u>Page No.</u>
1	EGRET SPACECRAFT - EXPLODED VIEW	4
2	CUT AWAY VIEW OF EXPLORER GAMMA RAY EXPERIMENT TELESCOPE (EGRET)	5
3	RECOMMENDED THERMAL DESIGN OF EGRET. PVT AND LIGHT SHIELD NOT SHOWN	11
4	MAXIMUM AND MINIMUM PERCENT SUNTIME ORBITS UTILIZED IN THERMAL DESIGN STUDIES OF EGRET	14
5	FOUR ORIENTATIONS OF EGRET IN THERMAL DESIGN STUDIES	15
6	SIMPLIFIED THERMAL MODEL OF HEAT TRANSPORT IN HIGH VOLTAGE STACK	19

FIGURES - APPENDIX A

1a	PICTORIAL VIEW OF THERMAL COMPUTER MODEL OF EGRET. PVT DOME AND LIGHT SHIELD NOT SHOWN	A-3
2a	NODE BAEDEKER FOR SPARK CHAMBER	A-4
3a	NODE BAEDEKER FOR HONEYCOMB/PRESSURE PLATE	A-5
4a	NODE BAEDEKER FOR PRESSURE VESSEL	A-6
5a	NODE BAEDEKER FOR POLYVINYL TOLUENE DOME	A-7
6a	NODE BAEDEKER FOR LIGHT SHIELD	A-8
7a	NODE BAEDEKER FOR EXTERIOR LAYER OF MLI THERMAL COVER	A-9

LIST OF FIGURES (Continued)

<u>Figure No.</u>		<u>Page No.</u>
8a	NODE BAEDEKER FOR MONOCOQUE SUPPORT STRUCTURE	A-10
9a	NODE BAEDEKER FOR ELECTRONICS COMPARTMENTS	A-11
10a	NODE BAEDEKER FOR VERTICAL SUPPORTS IN ELECTRONICS COMPARTMENTS	A-12
11a	NODE BAEDEKER FOR DEEP "I" BEAM CHANNELS ENCLOSING TOTAL ADSORPTION SHOWER COUNTER	A-13
12a	NODE BAEDEKER FOR TOTAL ABSORPTION SHOWER COUNTER (TASC)	A-14
13a	NODE BAEDEKER FOR EXTERIOR LAYER OF MLI ON SPACECRAFT	A-15

FIGURES - APPENDIX B

1b	SURFACE NOMENCLATURE FOR EXTERIOR GEOMETRIC MODEL OF EGRET	B-2
2b	SURFACE NOMENCLATURE FOR INTERIOR GEOMETRIC MODEL OF PRESSURE VESSEL	B-3
3b	SURFACE NOMENCLATURE FOR INTERIOR GEOMETRIC MODEL OF PRESSURE BULKHEAD	B-4
4b	SURFACE NOMENCLATURE FOR EXTERIOR GEOMETRIC MODEL OF HIGH VOLTAGE STACK	B-5
5b	SURFACE NOMENCLATURE FOR EXTERIOR LAYER OF MLI ON SPACECRAFT	B-6



## I. PURPOSE

The purpose of this report is to present the results of a thermal design analysis of the Explorer Gamma Ray Experiment Telescope (EGRET) and to provide GSFC with a document that defines the thermal computer model that was delivered as part of this effort. This report completes the stipulated requirements under Contract NAS5-23206.

## II. BACKGROUND

This study effort to define the thermal control subsystem of EGRET was undertaken and accomplished during a time in which the design of EGRET was undergoing revision. In particular, the type of mission adapter structure which joined EGRET to the transition ring of the Low Cost Modular Spacecraft (LCMS) was reconfigured from an open truss to a closed monocoque. This change was significant from a thermal viewpoint as all of the EGRET's radiators are located inside this support region. The mounting location of the electronics' boxes also changed as the design evolved.

The initial analyses were done with hand calculations and a thermal computer model of EGRET which had a detailed simulation of the upper region comprising the high voltage stack, pressure vessel, polyvinyl toluene (PVT) dome, light shield and the MLI system. The model of the lower region simulated all external EGRET radiators, the open truss support system plus that portion of the (insulated) spacecraft that had a direct view of EGRET. All EGRET component powers were applied directly to the radiators in this original model as each individual box was to be directly mounted on a radiator to minimize stack temperature gradients caused by the asymmetric box internal power dissipations. A parametric study of the stack and PVT dome temperature gradients was made using the initial computer model in parallel with an effort to develop a detailed model of the lower region of EGRET comprising the Total Absorption Shower Counter (TASC) with PMT'S plus all electronics compartments.

The external support structure change to a monocoque occurred at approximately the same time that the detailed internal thermal model of EGRET was finished so that a second set of parametric runs was made with the full thermal computer model using the new external and internal couplings. It is this second, full up thermal computer model that was delivered to GSFC as part of this effort.

Figure 1 is an exploded view of EGRET spacecraft and Figure 2 is a cutaway view of EGRET showing the arrangement of all internal components. The .1 inch thick aluminum (6061-T6) pressure vessel, which encloses the spark chamber stack assembly, contains neon gas under a pressure of 1.0-1.2 atmospheres. Exterior to the pressure vessel and in sequential order by increasing radius, there is a .6 inch thick anti-coincidence counter dome made of Polyvinyl Toluene (PVT), a .4 inch thick light shield comprising two 3 mil. aluminum face sheets separated by ECCOFOAM and an outer, multi-layer, insulation (MLI) thermal protection system. Below the pressure bulkhead, at the bottom of the spark chamber, is a Total Absorption Shower Counter (TASC) comprising a thirty inch diameter, 693 lbm. NaI crystal, with seven photomultiplier tubes (PMT's) surrounded by an annulus of electronics' boxes.

As part of the overall thermal design philosophy for the Low Cost Modular Spacecraft (LCMS) Program, the spacecraft is designed to be thermally isolated from the experiment payload. This design approach minimizes the heat exchange between the modular spacecraft and any particular experiment payload, thereby making the LCMS adaptable to a variety of experiment payloads with minimum impact on its thermal design. For this analysis, we have assumed a multi-layer insulation (MLI) blanket between the EGRET and an average spacecraft temperature of +10°C and the Mission Adapter has been treated as being conductively isolated from the spacecraft structure (transition ring).

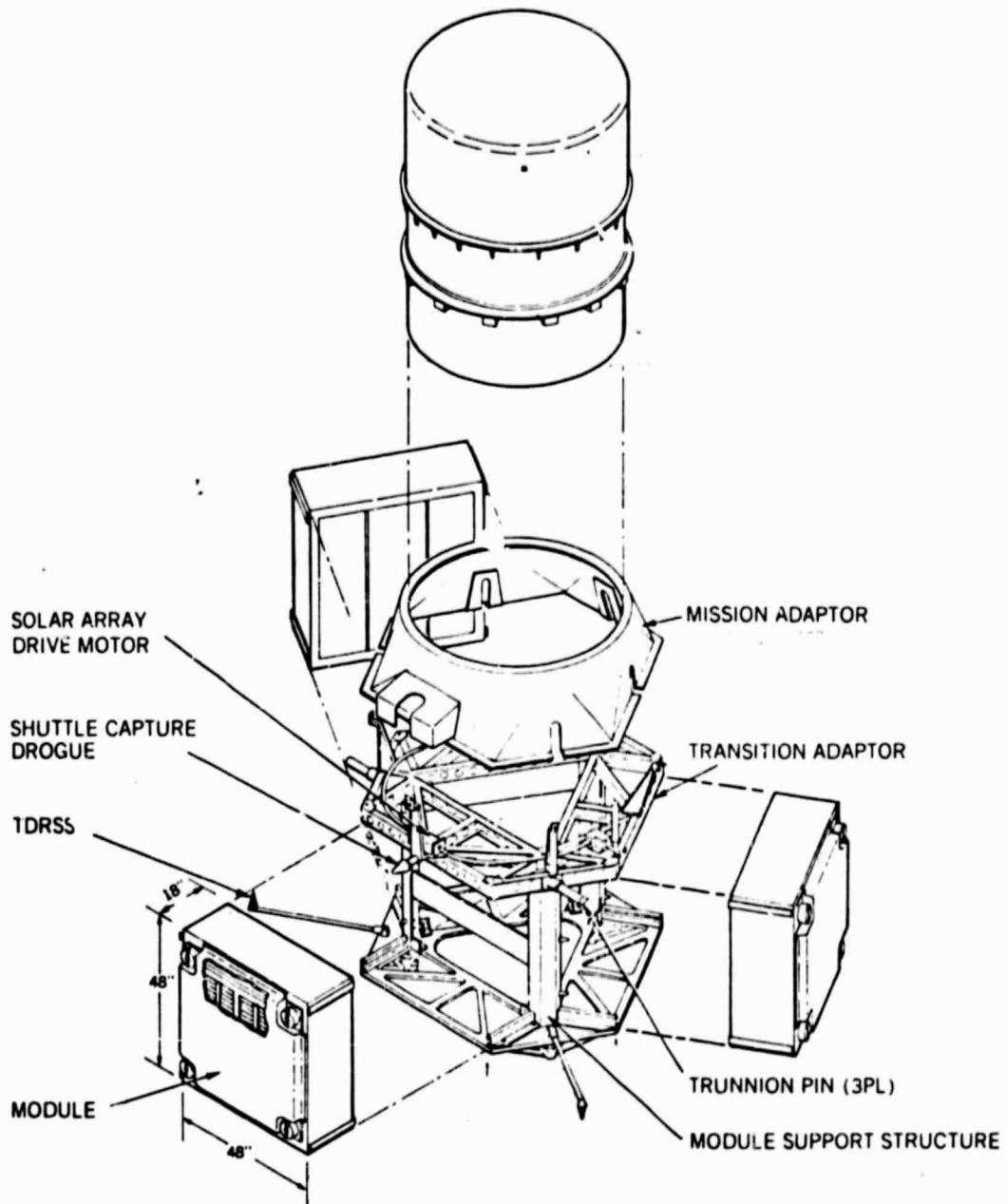


FIGURE 1 EGRET SPACECRAFT - EXPLODED VIEW

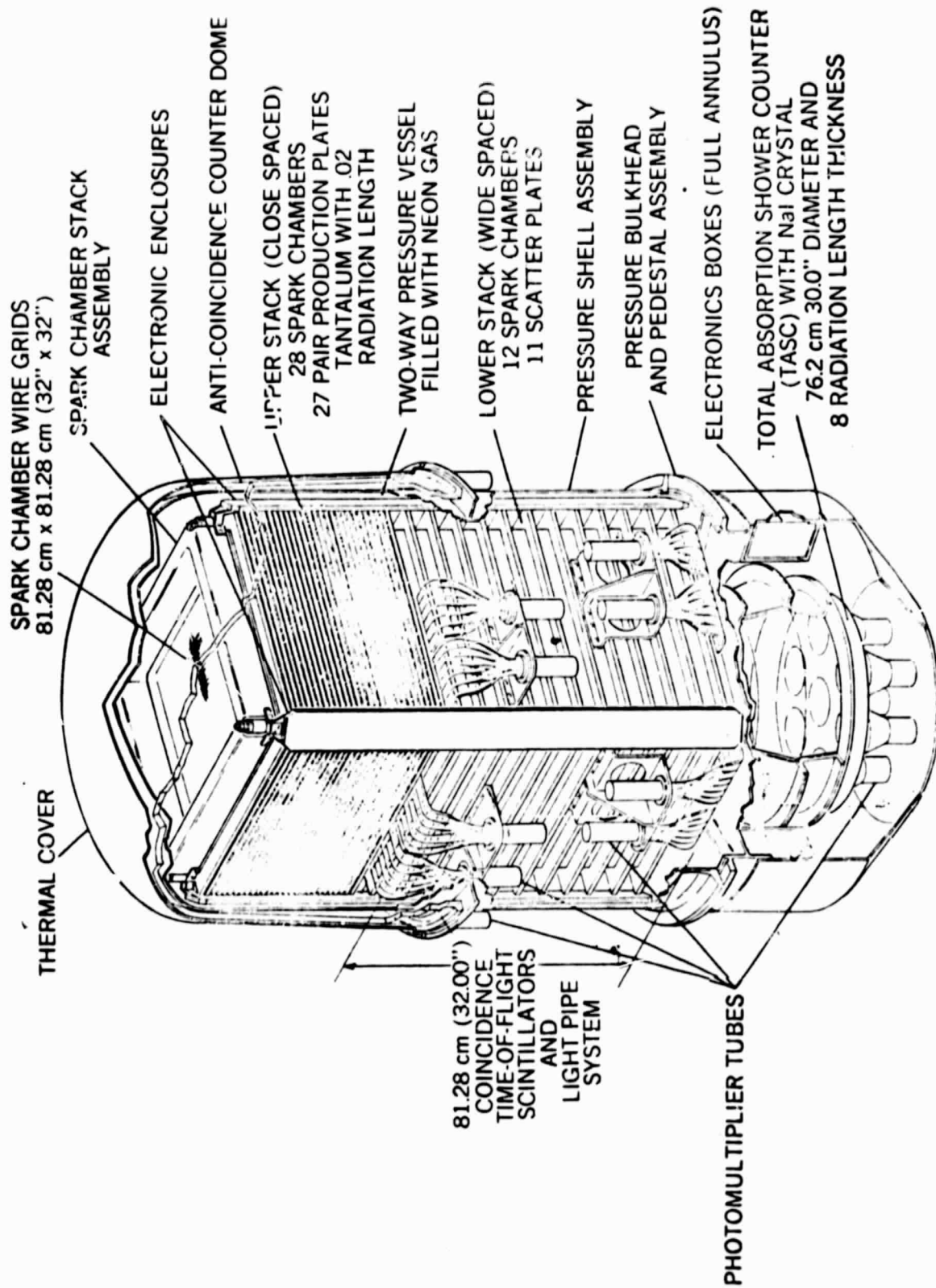


FIGURE 2 CUT-AWAY VIEW OF EXPLORER GAMMA RAY EXPERIMENT TELESCOPE (EGRET)

### III. RESULTS AND RECOMMENDATIONS

Table 1 summarizes the thermal design requirements for EGRET. The major thermal concern was the temperature distribution in the PVT dome as an earlier test at GSFC had shown that the material would fracture under thermal stress. The temperature gradient requirement of  $< 5^{\circ}\text{C}/\text{inch}$  for the PVT dome was a result of this earlier test.

In order to minimize the temperature gradients in the PVT dome, while attempting to control its temperature level to within  $-10^{\circ}\text{C}$  to  $+30^{\circ}\text{C}$  ( $-25^{\circ}\text{C}$  to  $+40^{\circ}\text{C}$  were allowable limits but  $-10^{\circ}\text{C}$  to  $+30^{\circ}\text{C}$  were ideal limits<sup>[1]</sup>), no heaters were conductively located near the PVT dome and the entire dome was radiatively coupled to the aluminum pressure vessel and, therefore, to the interior of EGRET, with high emittance surfaces. The IR emittance of polyvinyl toluene (transparent to the naked eye) was measured at GSFC to be 0.9 against both a high and low emittance background. Both the interior and exterior surfaces of the aluminum pressure vessel were assumed to be anodized ( $\epsilon = .84$ ) so that the dominant thermal coupling to the PVT dome was by radiation. The dome is mechanically and conductively mounted to a flange at its bottom perimeter; however, due to the low thermal conductivity of PVT ( $k = .0018 \text{ watt/cm} - ^{\circ}\text{C} = .104 \text{ Btu/Hr-Ft-}^{\circ}\text{R}$ ), there is a relatively short effective fin length (1.8 cm). In the thermal computer model, the spacing between the first three axial nodes in the PVT dome at the mounting flange is .5 inch and 1.0 inch so that simple temperature predictions from the model can be used to check on the  $< 5^{\circ}\text{C}/\text{inch}$  temperature gradient requirement.

The PVT dome is a scintillation detector and is externally surrounded by a light tight dome. The interior surface of the light shield is recommended to be buffed aluminum so as to have a low emittance surface facing the PVT dome ( $\epsilon \approx .05$ ) and the exterior surface of the light

---

[1] Written communication from J. Marshburn dated February 4, 1975.

<u>COMPONENT</u>	<u>TEMP. LEVEL</u>	<u>TEMP. GRADIENT</u>
OVERALL SYSTEM	10°C ± 20°C <sup>[1]</sup>	
PVT DOME	10°C ± 20°C (ideal) -25°C to 40°C (total) -50°C to 50°C (fatal)	< 5°C/inch
PMT's ON DOME	0°C ± 10°C	
HIGH VOLTAGE STACK		< 10°C LATERAL < 20°C AXIAL

[1] Temperature level changes must be < 10°C/hr.

TABLE 1 THERMAL REQUIREMENTS FOR EGRET

shield is to be covered with a multilayer insulation (MLI) system ( $\epsilon_{\text{MLI}} \leq .02$ ). Based upon a linearized radiation analyses, the radial thermal resistance of a relatively poor MLI system ( $\epsilon = .02$ ) is twenty times the radial (conductive) thermal resistance offered by the 1 centimeter thick ECCOFOAM filled lightshield.

The MLI blanket is an important part of the thermal design of EGRET because it both minimize the heater power required to provide temperature level control in the region of the high voltage stack and it also ameliorates the temperature gradient in the PVT dome due to asymmetric solar heating of the dome region. There is a total of approximately 96.8 square feet of MLI covering the EGRET and, assuming an effective emittance of  $\epsilon = .02$  with an interior temperature of  $10^{\circ}\text{C}$ , the total heat leak through the MLI to space is 66 watts (neglecting any environmental fluxes absorbed on the exterior layer of the blanket). An effective emittance of .01 would reduce this heat leak to 33 watts, well within the 50 watts of heater power budgeted for EGRET. Computer runs with the initial thermal model of EGRET showed that a change from  $\epsilon_{\text{MLI}} = .02$  to  $\epsilon_{\text{MLI}} = .01$  increased the average internal temperature by 6 to  $8^{\circ}\text{C}$  with all internal power and 50 watts of heater power on.

The outer layer of the MLI has been modeled as having an  $\alpha = .45$ ,  $\epsilon = .85$  to simulate 3 mil aluminized Kapton. A unique design requirement for this MLI system is that it must have a high degree of uniformity of total material thickness across the FOV of the gamma ray telescope. Preliminary design recommendations for this MLI system have been forwarded by GSFC. [2]

A dominant factor in the definition of the thermal design of EGRET is the large external surface areas on the experiment and the low internal power dissipation. There is approximately 96.8 square feet of exposed insulation on the upper region and another 28.4 square feet of area on the monocoque mission adaptor. The insulated upper portion is

---

[2] Letter from F. Ruccia of ADL to J. Marshburn of GSFC dated June 12, 1975.



under temperature level control by use of 50 watts of thermostatically controlled heater power.

The locations considered for these heaters have been on the pinch frame at the top of the stack and on the annular, exposed region of the pressure bulkhead at the bottom of the stack. Axial temperature gradients in the stack less than 20°C were predicted for all orbits/orientations considered; however, smaller axial gradients were predicted when the 50 watts of heaters were mounted to the bottom plate of the pressure vessel. This location would allow the heaters to be mounted outside the pressurized enclosure so that: 1) additional electrical (heater) wires would not have to penetrate the pressure vessel; and 2) outgassing of the heaters into the neon gas would not be a problem. Although not specifically analyzed in this current set of computer runs, we recommend that several sets of thermostatically controlled heaters be applied to the exterior of the bottom pressure plate, around the perimeter of the stack, such that the total dissipation of all heaters would be 50 watts. The spatial distribution of the individual heater circuits would compensate for the asymmetric power dissipation in the electronics' boxes currently mounted to the pressure bulkhead and provide a nearly uniform temperature on the lower pressure bulkhead. Additional analysis based upon the latest information as to where the individual boxes are located would be needed to size and locate the individual heater circuits. With the heaters located at the bottom end of the stack, the effectiveness of the MLI thermal protection system would have an important influence on the axial gradients in the PVT dome and stack as there is only 14.2 watts of power dissipation in the PMT's and high voltage connector strips inside the insulated boundaries. The temperature controlled pressure bulkhead comprises the only uninsulated boundary to the pressurized enclosure.

It is also feasible to consider using a heat pipe to isothermize the lower pressure bulkhead and electronics' compartments so that the number of individual thermostatically controlled heater circuits could be significantly reduced. Providing mechanical clearances for such a

circumferential heat pipe in this region appears to be a significant obstacle to this approach.

In the lower region of EGRET, below the pressure vessel boundary, there is approximately 47 watts of internal power dissipation in the electronics' boxes. If this power were radiated to space uniformly over the full area of the monocoque and the internal temperature were to be maintained at 10°C, then a uniform effective emittance of .05 would be needed over the exterior surface of the full monocoque. A typical uncertainty of  $\pm .02$  in this effective emittance would result in a temperature uncertainty of approximately  $\pm 35^\circ\text{C}$ . A thermal design that would be minimally influenced by variation in exterior optical properties is shown in Figure 3. Basically, most of the monocoque transition structure would be insulated on its exterior, leaving only 1.78 square feet uninsulated on the anti-sun side of EGRET (1/16 of the total area). Heat pipe(s) would be attached to the inside of the monocoque to absorb the power being radiated from the electronics boxes over a large, relatively uniform, temperature area and conduct it to the single space viewing radiator. The average temperature difference between EGRET and its isothermal mission adaptor would be 4°C. An alternative thermal design approach would be to mount the heat pipe(s) directly to the basic structure of EGRET, the same structure that holds the electronics boxes, conductively isothermalize this portion of EGRET with the heat pipe(s), and then radiate to the interior of the closed monocoque over a limited area on the anti-sun side of the spacecraft. The advantage of this second approach would be that the heat pipe would be used to isothermalize the EGRET structure directly while the disadvantage would be the large circumferential temperature gradients in the monocoque support structure because a colder, and, therefore, larger effective radiating area viewing space would be needed, to set up the approximately 32°C temperature difference between the EGRET electronics bays and a 3.55 square foot radiator (one-eighth of the total area overall). The internal ( $\mathcal{F}$ ) radiative coupling was assumed to be .82. At -22°C the radiator would need an exterior effective emittance of approximately .63.

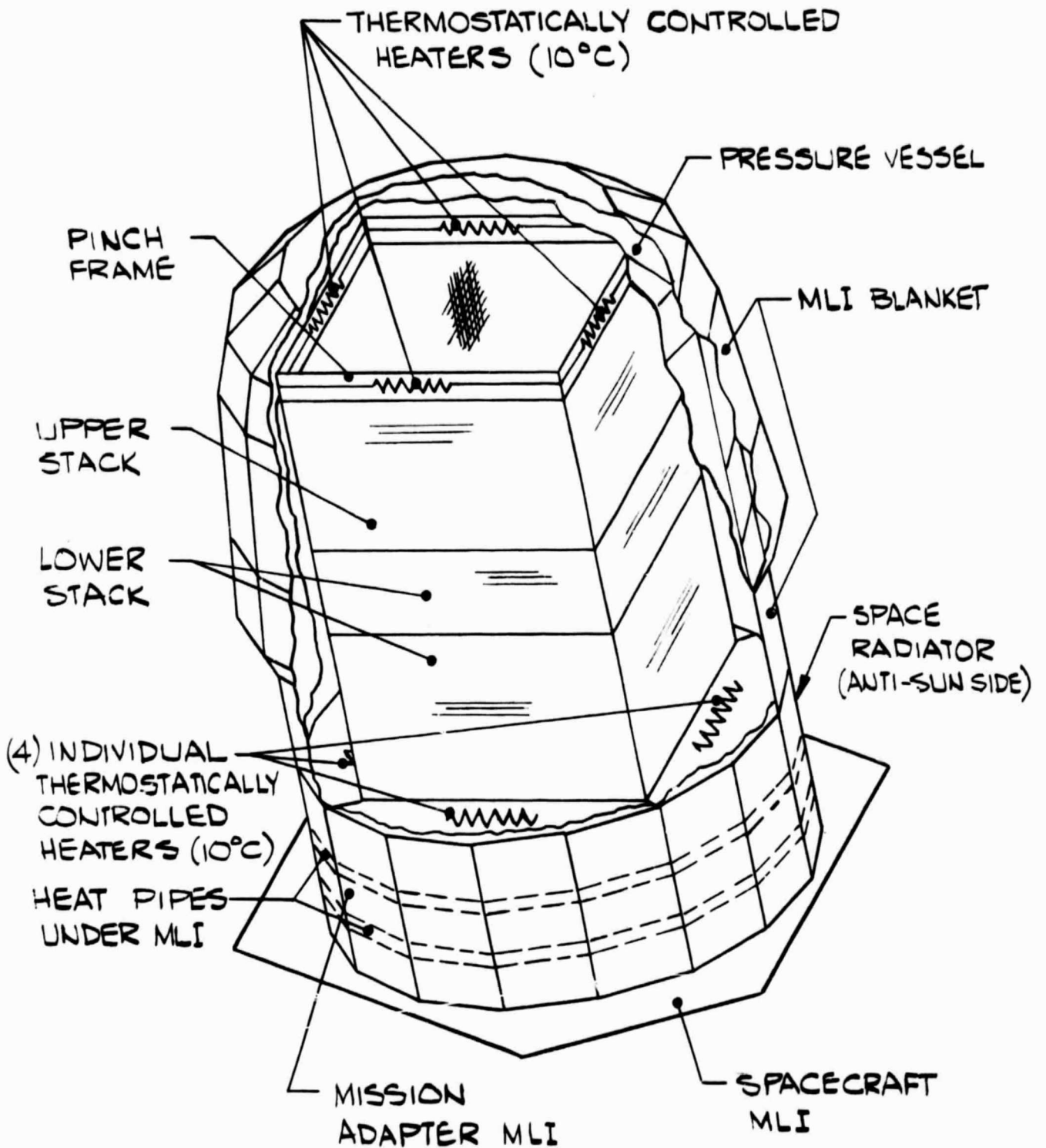


FIGURE 3 RECOMMENDED THERMAL DESIGN  
OF EGRET  
PVT DOME AND LIGHT SHIELD  
NOT SHOWN

## COMPUTER MODEL RESULTS

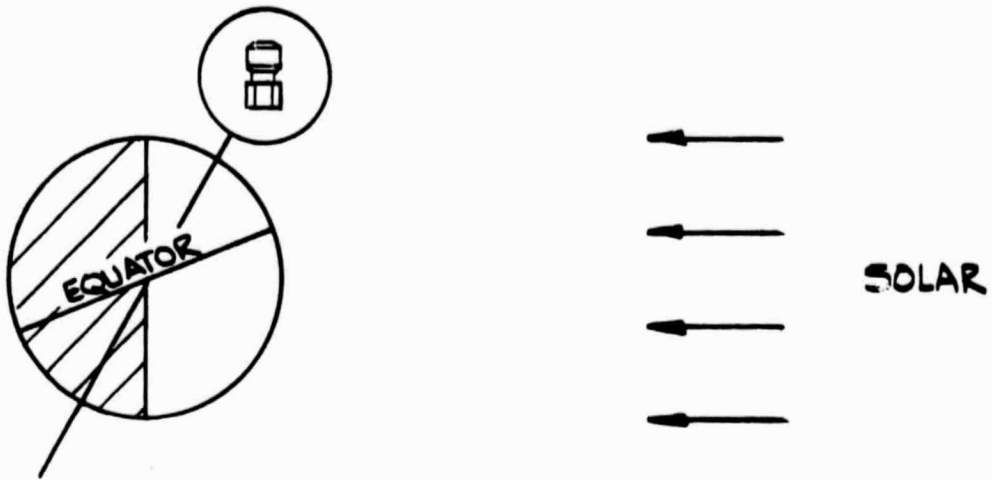
A 241 node thermal computer model of EGRET was developed and exercised for a range of orbits/spacecraft orientations and internal power dissipations to test the validity of the thermal design as discussed. The details of the computer model are described in the next section of this report and both the node baedeker and also the CONSHAD numerical surface names are tabulated in the Appendixes.

Table 2 summarizes the orbital/thermal parameters utilized in the computer studies and Figure 4 shows the maximum and minimum percent suntime orbits for the determination of hot and cold case boundary conditions. Figure 5 shows the four orientations of EGRET with respect to the solar vector that were used in the analysis. The maximum projected area of the dome was calculated to occur at a dome tip angle of  $32.8^\circ$  toward the sun. Table 3 summarizes the temperatures predicted for the various conditions of EGRET orientations, percent suntime orbit and internal power dissipations. The difference in internal power dissipation between instrument "on" and instruments "off" was 47 watts, in these runs. With the exception of the  $0^\circ\text{C} \pm 10^\circ\text{C}$  requirement for the PMT's on the PVT dome, all regions of EGRET are predicted to run within their specified temperature limits when both instrument and heater power were "on." The PMT's have a maximum predicted temperature of  $14.5^\circ\text{C}$ .

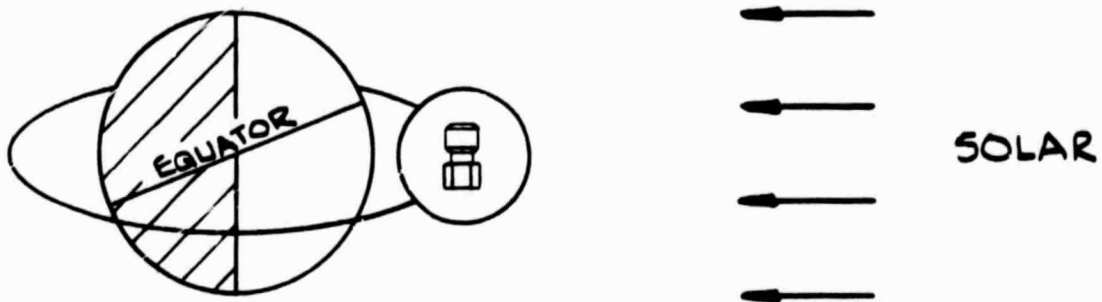
With the 50 watts of heater power "off" inside the gas-filled pressure vessel, the average dome and stack temperature is a function of EGRET's projected area to the sun, with average temperature less than  $-10^\circ\text{C}$  being predicted for the two orientation of dome top and aft end to sun. With both internal power and heater power off, EGRET has a minimum predicted temperature level of  $-68^\circ\text{C}$  with the  $+10^\circ\text{C}$  spacecraft end looking at the sun in the maximum percent suntime orbit. The recommended procedure for on-orbit operations will be to keep all internal power dissipations on all of the time.

SOLAR CONSTANT	429.2 BTU/HR-FT <sup>2</sup>	(.1353 w/cm <sup>2</sup> )
ALBEDO	0.30	
EARTH IR	75.18 BUT/HR-FT <sup>2</sup>	(.0237 w/cm <sup>2</sup> )
ALTITUDE (NM)	300	
ORBIT INCLINATION (°C)	33	

TABLE 2 ORBITAL/ENVIRONMENTAL PARAMETERS AREA  
IN EGRET THERMAL COMPUTER MODEL STUDIES

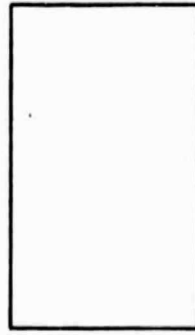
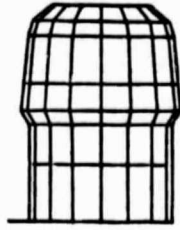
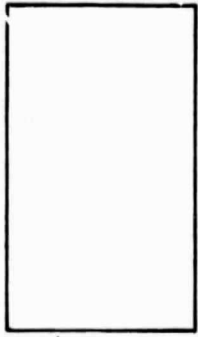


a) MAXIMUM PERCENT SUNTIME ORBIT (75%)

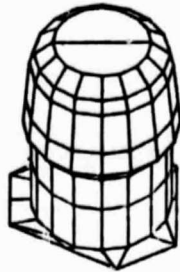
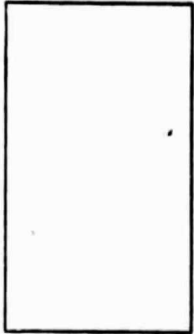


b) MINIMUM PERCENT SUNTIME ORBIT (63%)

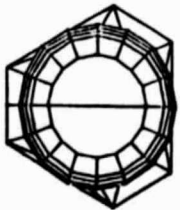
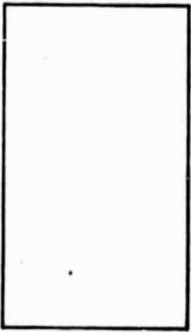
FIGURE 4 MAXIMUM AND MINIMUM PERCENT SUNTIME ORBITS UTILIZED IN THERMAL DESIGN STUDIES OF EGRET



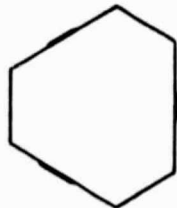
a) SIDE TO SUN



b) MAXIMUM PROJECTED AREA



c) DOME TOP TO SUN



d) AFT END TO SUN

FIGURE 5 FOUR ORIENTATIONS OF EGRET IN THERMAL DESIGN STUDIES

ORIENTATION	% SUNTIME	INTERNAL POWER		PVT DOME			AVG. T °C	
		INSTRUMENTS	HEATERS	AVG. T °C	MAX ΔT °C	MAX GRADIENT °C/INCH		
MAXIMUM PROJECTED AREA ↓	MIN	ON	ON	14	9.30	0.41	14.8	
	↓	↓	OFF	OFF	-11	3.27	0.13	-10.6
		↓	OFF	ON	-7	10.13	0.52	-7.2
		↓	↓	OFF	-39	4.22	0.23	-39.4
		MAX	ON	ON	14	9.80	0.45	15.3
		↓	↓	OFF	-10	4.40	0.19	-10.0
		↓	OFF	ON	-7	10.70	0.58	-6.6
		↓	↓	↓	OFF	-37	5.53	0.30
SIDE TO SUN ↓	MIN	ON	ON	14	8.66	0.42	15.6	
	↓	↓	OFF	OFF	-10	3.31	0.14	-9.7
		↓	OFF	ON	-6	9.37	0.53	-6.3
		↓	↓	OFF	-37	4.17	0.25	-38.2
		MAX	ON	ON	15	9.04	0.48	15.1
		↓	↓	OFF	-10	4.48	0.21	-10.3
		↓	OFF	ON	-7	8.99	0.59	-6.9
		↓	↓	↓	OFF	-37	5.50	0.32
DOME TOP TO SUN ↓	MIN	ON	ON	10	9.58	0.35	8.7	
	↓	↓	OFF	OFF	-18	2.21	0.40	-18.3
		↓	OFF	ON	-15	10.72	0.47	-14.8
		↓	↓	OFF	-49	2.96	0.12	-50.1
		MAX	ON	ON	11	9.77	0.36	11.8
		↓	↓	OFF	-14	2.64	0.05	-14.3
		↓	OFF	ON	-11	10.79	0.47	-10.9
		↓	↓	↓	OFF	-44	3.43	0.13
AFT END TO SUN ↓	MIN	ON	ON	0	8.46	0.33	0.4	
	↓	↓	OFF	OFF	-30	1.04	0.10	-29.3
		↓	OFF	ON	-25	9.40	0.39	-25.7
		↓	↓	OFF	-66	0.20	0.01	-66.9
		MAX	ON	ON	0	8.32	0.28	-2.0
		↓	↓	OFF	-31	1.07	0.12	-30.1
		↓	OFF	ON	-25	9.15	0.37	-26.4
		↓	↓	↓	OFF	-68	0.40	0.03
SIDE TO SUN (Heaters at the Bottom of the Stack)	MIN	ON	ON	9	3.13	0.15	10.7	
	MAX	ON	ON	9	3.94	0.13	10.3	

TABLE 3 TEMPERATURE PREDICTIONS (°C) USING EGRE



PVT DOME		STACK			PMT (PVT DOME)		NaI CRYSTAL	ELECTRONICS	
MAX $\Delta T$ °C	MAX GRADIENT °C/INCH	AVG. T °C	MAX LATERAL $\Delta T$ °C	MAX AXIAL $\Delta T$ °C	MAX T °C	MIN T °C	AVG. T °C	MAX T °C	MIN T °C
9.30	0.41	14.8	1.45	8.50	13.7	11.8	8.3	8.4	6.5
3.27	0.13	-10.6	0.79	0.77	-10.0	-12.3	-11.4	-11.1	-12.9
10.13	0.52	- 7.2	1.39	10.03	- 7.8	- 9.7	-14.3	-14.4	-15.3
4.22	0.23	-39.4	0.68	1.13	-37.8	-40.2	-40.2	-40.2	-40.8
9.80	0.45	15.3	1.67	8.71	14.5	12.1	8.5	8.7	6.6
4.40	0.19	-10.0	1.03	1.06	- 9.1	-12.0	-11.1	-10.8	-12.6
10.70	0.58	- 6.6	1.63	10.27	- 6.8	- 9.4	-14.0	-14.1	-15.1
5.53	0.30	-38.7	0.92	1.46	-36.6	-39.8	-39.8	-39.7	-40.4
8.66	0.42	15.6	0.95	8.03	14.8	12.6	9.3	9.3	7.5
3.31	0.14	- 9.7	0.83	0.29	- 8.8	-11.4	-10.3	- 9.9	-11.7
9.37	0.53	- 6.3	1.40	9.47	- 6.5	- 8.7	-13.1	-13.1	-14.1
4.17	0.25	-38.2	0.58	0.54	-36.2	-39.0	-38.7	-38.6	-39.2
9.04	0.48	15.1	1.68	8.20	14.7	11.9	8.6	8.8	6.7
4.48	0.21	-10.3	1.03	0.43	- 9.0	-12.3	-11.1	-10.7	-12.6
8.99	0.59	- 6.9	1.63	9.70	- 6.7	- 9.6	-14.0	-14.0	-15.0
5.50	0.32	-39.2	0.75	0.76	-36.6	-40.3	-40.0	-40.7	-40.5
9.58	0.35	8.7	0.89	9.01	6.7	6.5	2.2	2.3	0.6
2.21	0.40	-18.3	0.23	0.99	-18.9	-19.6	-19.0	-18.6	-20.2
10.72	0.47	-14.8	0.21	10.71	-16.7	-17.1	-22.0	-22.3	-22.8
2.96	0.12	-50.1	0.12	1.35	-50.1	-50.3	-50.8	-51.0	-51.1
9.77	0.36	11.8	0.93	9.00	9.8	9.1	5.1	5.3	3.6
2.64	0.05	-14.3	0.26	1.15	-15.0	-15.7	-15.2	-14.8	-16.4
10.79	0.47	-10.9	0.88	10.63	-12.8	-13.1	-18.1	-18.5	-18.9
3.43	0.13	-44.4	0.17	1.55	-44.5	-44.7	-45.3	-45.4	-45.6
8.46	0.33	0.4	0.80	8.41	- 1.7	- 2.3	- 5.5	- 5.4	- 7.1
1.04	0.10	-29.3	0.20	0.48	-30.0	-30.6	-29.1	-28.7	-30.2
9.40	0.39	-25.7	0.74	10.23	-27.7	-28.1	-32.3	-32.6	-33.0
0.20	0.01	-66.9	0.03	0.11	-66.9	-67.0	-66.5	-66.6	-66.8
8.32	0.28	- 2.0	0.83	8.33	- 2.3	- 2.4	- 6.0	- 5.8	- 7.6
1.07	0.12	-30.1	0.23	0.61	-30.8	-31.4	-29.7	-29.3	-30.9
9.15	0.37	-26.4	0.77	10.16	-28.5	-28.7	-33.0	-33.3	-33.6
0.40	0.03	-68.1	0.04	0.26	-68.1	-68.3	-67.6	-67.7	-67.9
3.13	0.15	10.7	0.96	1.04	11.4	8.9	11.2	11.5	9.5
3.94	0.13	10.3	1.06	0.91	11.3	8.2	10.5	10.9	8.7

TEMPERATURE PREDICTIONS (°C) USING EGRET THERMAL COMPUTER MODEL

#### IV. DESCRIPTION OF THERMAL COMPUTER MODEL

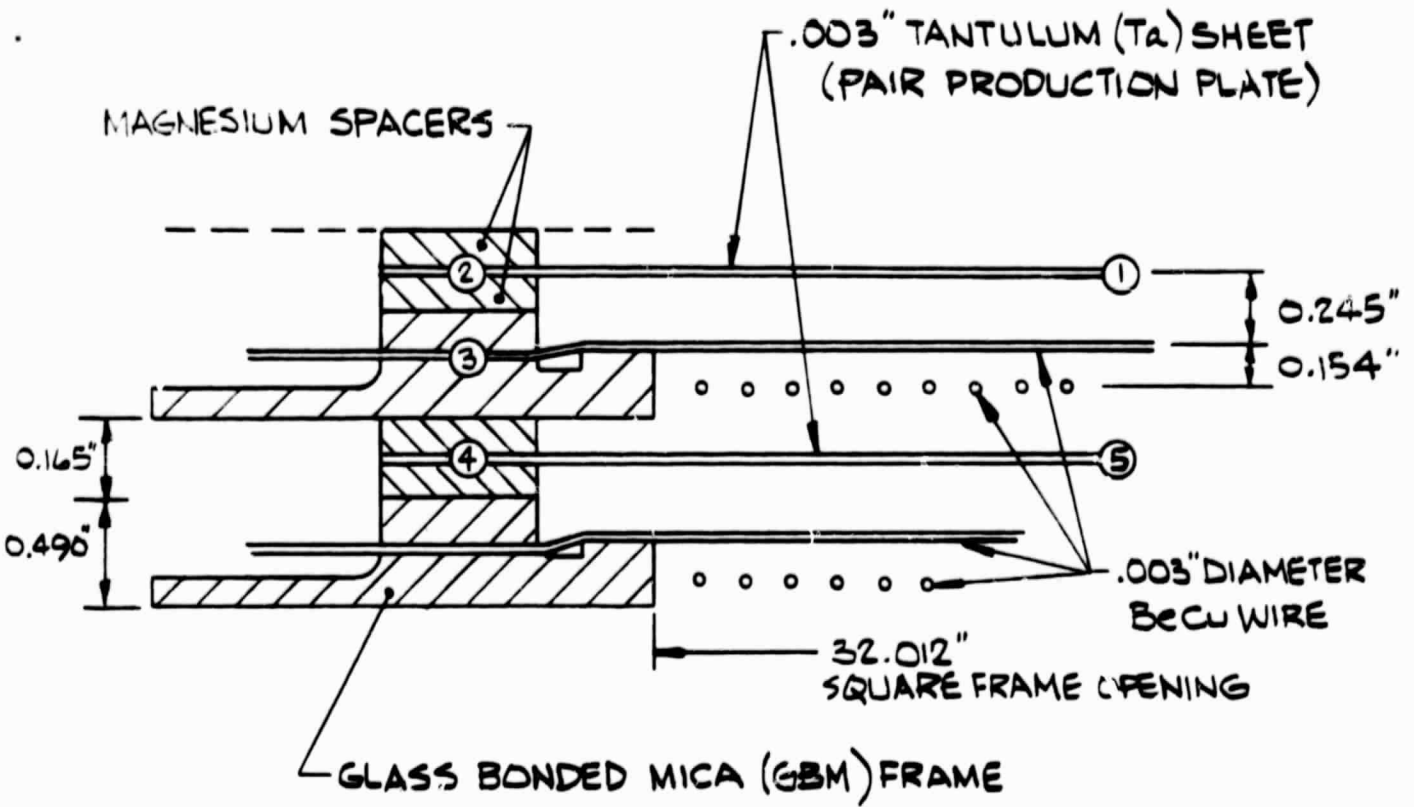
This section contains a discussion of the methods used to develop the conductive and radiative couplings for the thermal computer model of EGRET. The discussion is keyed to the node numbers shown in Appendix A and all thermophysics properties used in the calculations are shown in Table 4. Because the thermal conductivity of polyvinyl toluene was of primary importance in determining the gradients in the anti-coincidence counter dome, and no values were found in the literature, Dynatech was subcontracted to measure its value. Appendix C contains a copy of the report received from Dynatech, documenting a measured value of .0018 w/cm K for the thermal conductivity of PVT at 40°C.

#### SPARK CHAMBER

One of the thermal design requirements for EGRET was that the temperature differences in the stack should ideally be less than 10°C laterally and less than 15°C to 20°C axially. In addition to designing EGRET so that the thermal boundary conditions external to the stack would be as uniform as possible, the modes of heat transport inside the stack were examined during the development of the thermal computer model to determine their significance on ameliorating any temperature gradients within the stack. The simplified model used to examine internal axial modes of heat transport is shown in Figure 6 as a cross section between two parallel tantalum sheets (pair production plates) sandwiched between glass bonded mica and magnesium spacers. There were three modes of transport considered to axially transfer heat between two adjacent pair production plates: 1) gas conduction in the neon, 2) direct radiative exchange between parallel plates ( $\epsilon = .05$ ) having an unobstructed view of each other, and 3) conduction from a plate to its perimeter, down through the spacers and glass bonded mica frame and back into the next tantalum sheet. The relative values of the thermal resistance of these three modes at 10°C is as follows:

MATERIAL	$\rho$ lbm/in <sup>3</sup>	$C_p$ BTU/lbm-°R	$\kappa$ BTU/hr-ft-°R	$\alpha$	$\epsilon$
Aluminum (6061-T6)	.098	.23	89.5	-	.05
Aluminized Kapton (3 mil)	-	-	-	.45	.85
Eccofgam	.001	.25	.012	-	-
Glass bonded mica	-	-	.233	-	-
Magnesium	.064	.25	45	-	.13
MLI	-	-	-	-	.01/.02
NaI	.132	.087	2.008	-	-
Neon (1 atm)	.0325 x 10 <sup>-3</sup>	-	.027	-	-
Polyvinyl Toluene	-	.25	.104	-	.90
Tantalum	.527	.035	20	-	0.05
Titanium	.163	.125	10	-	.31

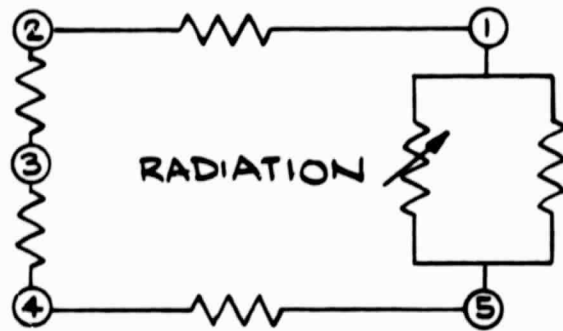
TABLE 4 THERMOPHYSICAL AND OPTICAL PROPERTIES OF MATERIALS USED IN EGRET THERMAL COMPUTER MODEL



Mg. SPACER

GBM FRAME

Mg. SPACER



PAIR PRODUCTION PLATE (Ta SHEET)

Ne GAS CONDUCTION

PAIR PRODUCTION PLATE (Ta SHEET)

FIGURE 6 SIMPLIFIED THERMAL MODEL OF HEAT TRANSPORT IN HIGH VOLTAGE STACK

Gas Conduction (Neon)	1°C/watt
Direct Radiation ( $\epsilon = .05$ )	11°C/watt
Conduction through Frame	21°C/watt

Because of the complexities involved in analyzing the details of the true heat transfer mechanisms inside the stack, the computer model was developed assuming no internal heat transfer inside the stack. The results of the computer run showed that temperature gradient requirements in the stack could be met with this conservative assumption and, therefore, real temperature gradients would be less than predicted gradients due to the internal heat transfer. The only nodes in the computer model representing the high voltage stack are for its perimeter of glass bonded mica and magnesium spacers and these nodes are conductively tied to each other and radiatively coupled to the enclosure interior to the pressure vessel. An emittance of 1.0 was used for the exterior surface of the high voltage stack due to the irregular surface with its associated radiation cavity effects. The PMT's were modeled as power sources (.1 watt each) on the side nodes of the high voltage stack and six line nodes, at two opposite corners of the stack (nodes 201-206), were utilized to simulate the power sources representing the high voltage connector strips. Axial conduction through the four titanium rods holding the stack together were neglected in the thermal computer model.

The three axial regions of the spark chamber telescope in the computer model were divided so as to coincide with the natural division between the upper and lower modules of the spark chamber and also to coincide with the line of the exterior flange on the pressure vessel which serves as a circumferential boundary for nodes on the pressure vessel wall. The interior surface of the 0.1 inch thick anodized aluminum pressure vessel directly views the exterior surface of the high voltage stack across a relatively narrow neon gas filled gap. Only radiative heat transfer was modeled across this gap, i.e., gas conduction was neglected.

#### HONEYCOMB PRESSURE PLATE

The 1 1/2 inch thick honeycomb pressure plate represented by nodes 39 and 40 was modeled as an axial conductive coupling of  $10 \text{ BTU}/\text{Hr}\text{-Ft}^2$  between face sheets. Lateral conductive couplings between node 39 and nodes 1-4 were based upon a continuous .1 inch thick aluminum plate. There was no lateral conductive coupling to node 40, the bottom face sheet of the honeycomb. As was the case of the couplings between the glass bonded mica and the magnesium spacer, thermal contact resistance between the bottom of the spark chamber stack (glass bonded mica) and the pressure plate was neglected in the thermal computer model.

#### TOTAL ABSORPTION SHOWER COUNTER

The TASC assembly shown in Figure 12a (Appendix A) is an aluminum housing structure containing a sodium iodine crystal. The structure is supported by a flange which is at the mid-section of the assembly and is hard connected to the surrounding TASC box shown in Figure 11a. The union of the TASC assembly and the box is accomplished at nodes 222 through 225. The top surface of the TASC assembly consists of an "as is" aluminum surface with a radiative coupling to the bottom of the honeycomb suspended beneath the pressure plate of the upper half of the experiment. Nodes in the TASC assembly are both conductively coupled via the aluminum structure and via heat flows internal to the NaI crystal. The PMT assembly was radiatively modeled as part of nodes 265 and 268, with node 231 as the bottom of the TASC containing the heat capacity and heat input of the seven PMT's.

The thermal conductance within each PMT tube was assumed to be sufficiently great, compared to radiative couplings in the lower half of the experiment, so that all the radiative couplings between the PMT tubes and the sidewalls of the surrounding box were modeled as couplings to the bottom of the NaI crystal. The radiative couplings were determined from data provided by NASA GSFC in the form of view factors between the various walls and surfaces. These values were multiplied by .724 for an effective  $\mathcal{F}$  between closely spaced anodized aluminum surfaces ( $\epsilon = .84$ ).

## LOWER BOX AND ELECTRONICS' COMPARTMENTS

The Lower Box and Electronics' Compartments is an aluminum structure with wall thickness varying between .5 and .8 cm, depending on the location. The TASC flange is hardcoupled to the wall of the box and the radial thermal resistivity across the width of the flange has been neglected. The nodal breakdown for the Lower Box is shown in Figure 11a and the Electronics' Compartments are shown in Figures 9a and 10a. Conductances were calculated based on the dimensions shown in the section drawing of the lower half of the EGRET experiment provided by NASA Goddard. The details of these calculations have been provided under separate cover.

The black body radiative couplings of the box to the TASC assembly and to the webs and outer wall were provided by NASA Goddard and these  $F$  values were multiplied by .724 to represent the effective  $\bar{F}$  between anodized aluminum surfaces. The radiative couplings between the nodes shown in Figure 11a and the webs running between the box and the outer wall, were calculated by summing the appropriate view factors in adjacent instrument bays. This was necessary because we have eliminated alternate web structures in the computer model to reduce the number of nodes in the final model. There are sixteen radial webs in the space between the Lower Box and the outer wall. We have simulated only eight of these webs in the computer model. While this approximation adds to the difficulty of calculating the radiative and conductive couplings in the lower half of the experiment, it was utilized in order to maintain an eight-fold symmetry so that the number of conductive connections formed at the pressure plate and web intersection would be reduced. Therefore, only webs which intersected the center of the pressure plate nodes, of which there eight, were used (nodes 253-260 in Figure 10a). The added complication of ignoring every other web in the housing structure meant that radiative and conductive paths normally coupled to two of the webs had to be lumped into a single web node.

In the case of the conduction paths, it was assumed that the eight webs used in the model were double the thickness of the sixteen actual webs in the experiment. The calculation of the effective  $A\bar{F}$  between the

two webs with nodal assignments were done by calculating the  $A\bar{F}$  from each of the node webs to the phantom web interceding them and using a series relation for radiative coupling which results in an effective  $A\bar{F}$  equal to the product of the two  $A\bar{F}$ 's calculated divided by the sum of the two.

The details of all of the conductive calculations throughout EGRET have been provided to GSFC under separate cover. Table 5 summarizes the internal power dissipations of EGRET by component and node number in the computer model. Appendix A contains a series of twelve figures showing the location of all nodes in the EGRET thermal model as delivered. Appendix B contains a series of figures showing the numerical surface names given to each surface in the geometric data developed for the CONFAC, SHADOW, and ORBITAL HEAT FLUX computer programs.



<u>COMPONENT</u>	<u>NODE</u>	<u>POWER (WATTS)</u>
Digital Housekeeping	31	1.0
	38	1.0
Time of Flight	32	7.5
Anti-Coincidence	33	7.5
Data Multiplexer	34	1.0
	35	1.0
Low Voltage Readout - I	34	3.0
- II	38	3.0
Power Supplied	36	10.0
	37	10.0
Stanford (TASC)	TBD	5.0
PMT's - PVT Dome (24)	111	0.6
	113	0.6
	115	0.6
	117	0.6
- Spark Chamber (18)	5	.225
	6	.225
	7	.225
	8	.225
	9	.225
	10	.225
	11	.225
	12	.225
- TASC (7)	231	.7
High Voltage Connectors	201	2.0
	202	2.0
	203	1.0
	204	1.0
	205	2.0
	206	2.0

TABLE 5 POWER DISSIPATIONS (WATTS) FOR EGRET

APPENDIX A

NODE BAEDEKER FOR THE EGRET THERMAL COMPUTER MODEL

<u>NODE NO.</u>	<u>DESCRIPTION</u>
1-16	Spark Chamber - Glass Bonded Mica Frame
17-20	Spark Chamber - Pinch Frame
21	Spark Chamber - Top Tantalum Sheet
22	Spark Chamber - Bottom Tantalum Sheet
31-40	Pressure Plate with Honeycomb
41-57	Pressure Vessel
61-109	Polyvinyl Toluene Dome
111, 113, 115, 117	Mounting Flange
119-144	Light Shield
151-167	Exterior Layer of MLI Blanket on Dome
171-178	Exterior Surfaces of Electronics' Compartments
179-186	Monocoque Mission Adaptor
187-190	Flange - Pressure Vessel to Pressure Plate
191-198	Exterior Layer of MLI Blanket on Spacecraft
201-206	Spark Chamber - High Voltage Connector Strips
211-212	Solar Paddles
213	Spacecraft (10°C)
214	Space (OK)
215-231	Total Absorption Shower Counter (TASC)
232-252	Deep "I" Beam Channel Enclosing TASC
253-260	Vertical Supports in Electronics' Compartments
265-268	PMT's on TASC
278-285	Reserved for Electronics' Compartments

Table 1a      NODE BAEDEKER FOR EGRET THERMAL  
COMPUTER MODEL

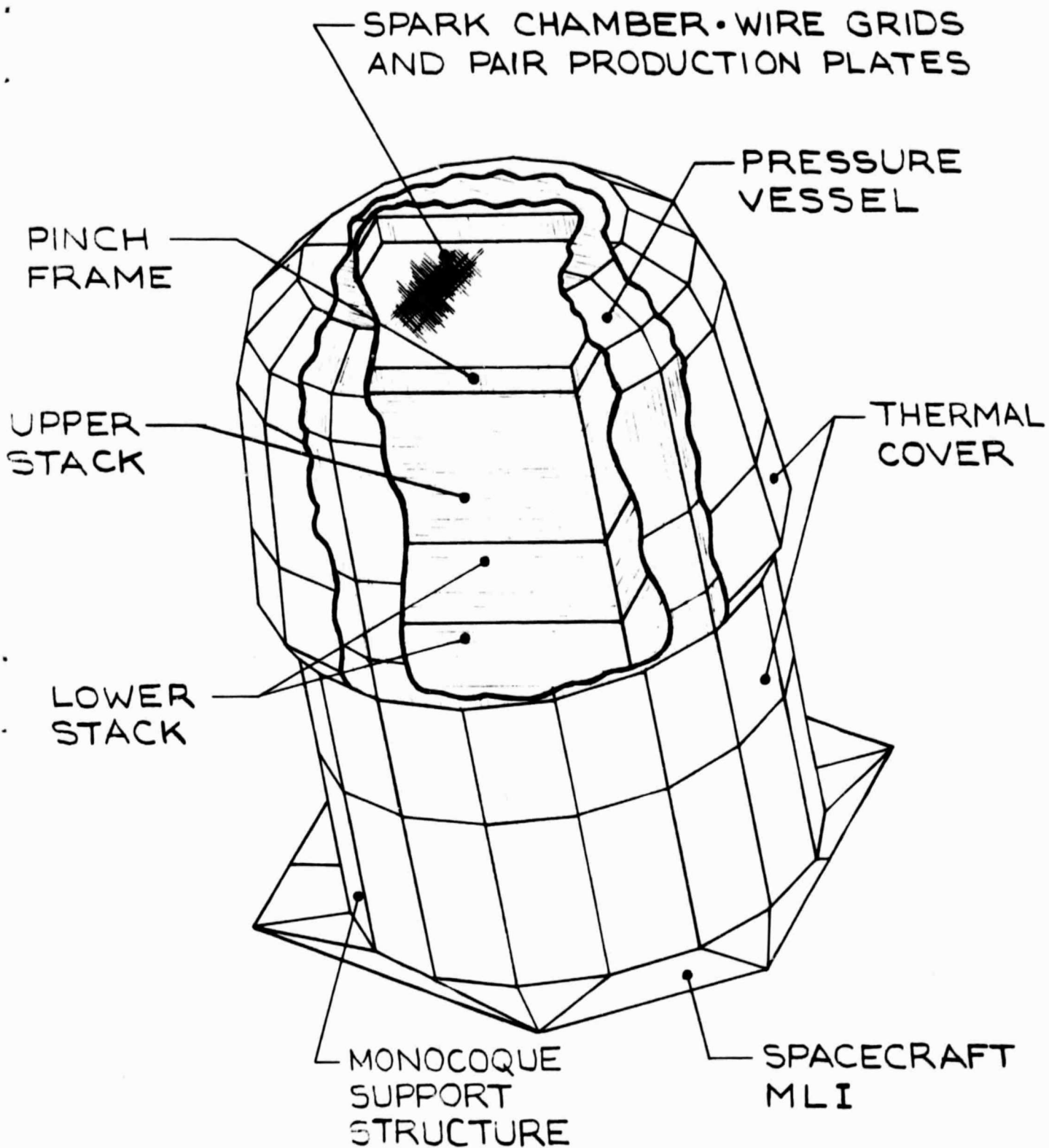


FIGURE 1a. PICTORIAL VIEW OF THERMAL  
COMPUTER MODEL OF EGRET.  
PVT DOME AND LIGHT SHIELD  
NOT SHOWN.

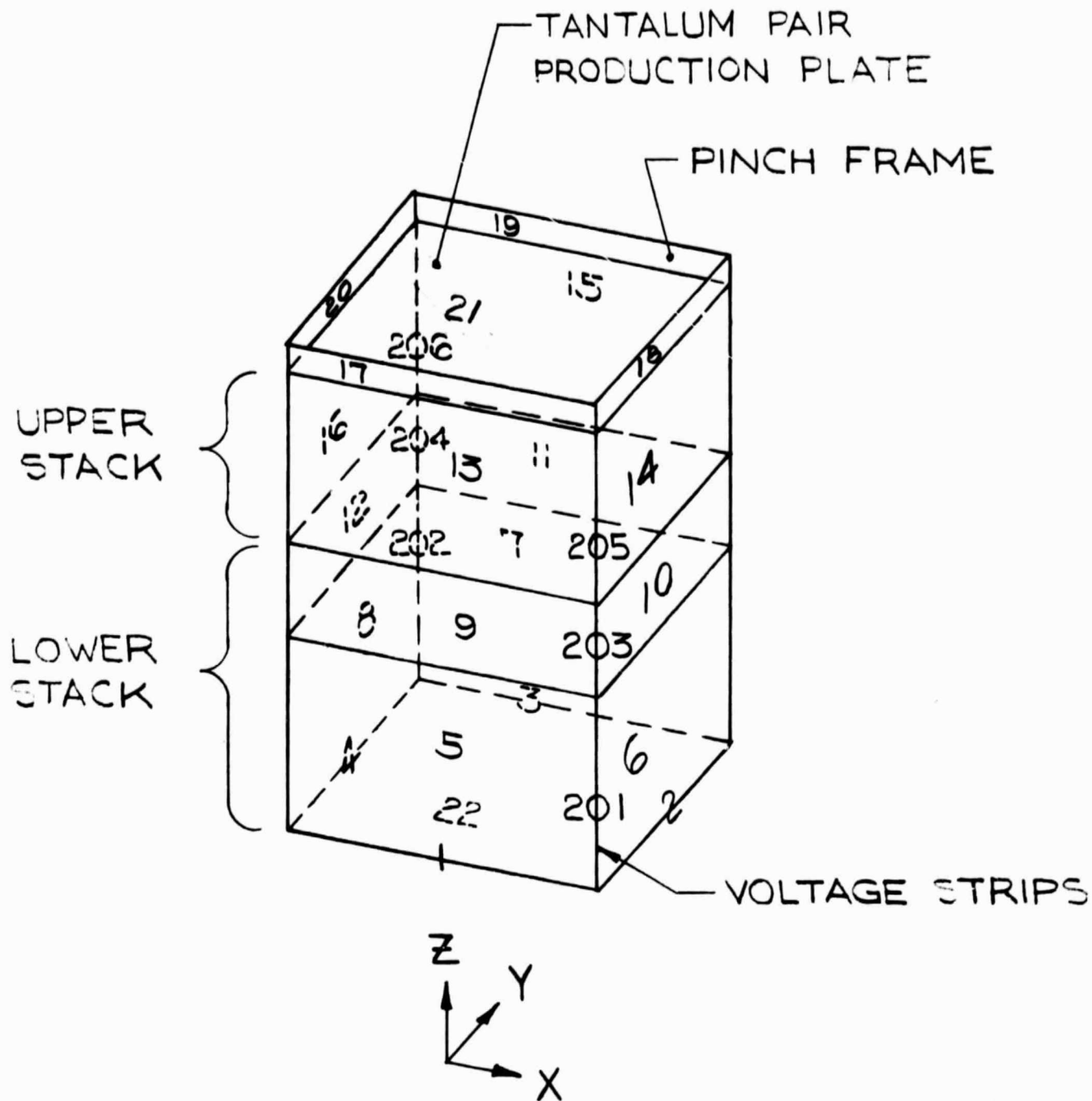


FIGURE 2a. NODE BAEDEKER FOR SPARK CHAMBER

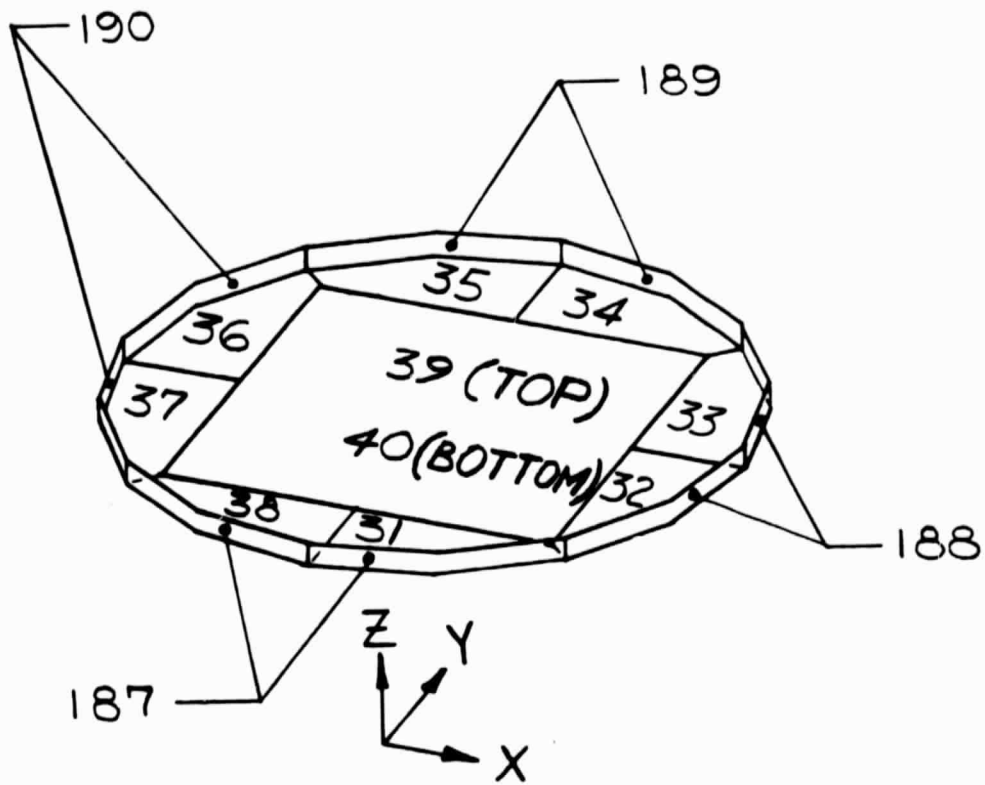


FIGURE 3a. NODE BAEDEKER FOR  
HONEYCOMB/PRESSURE PLATE

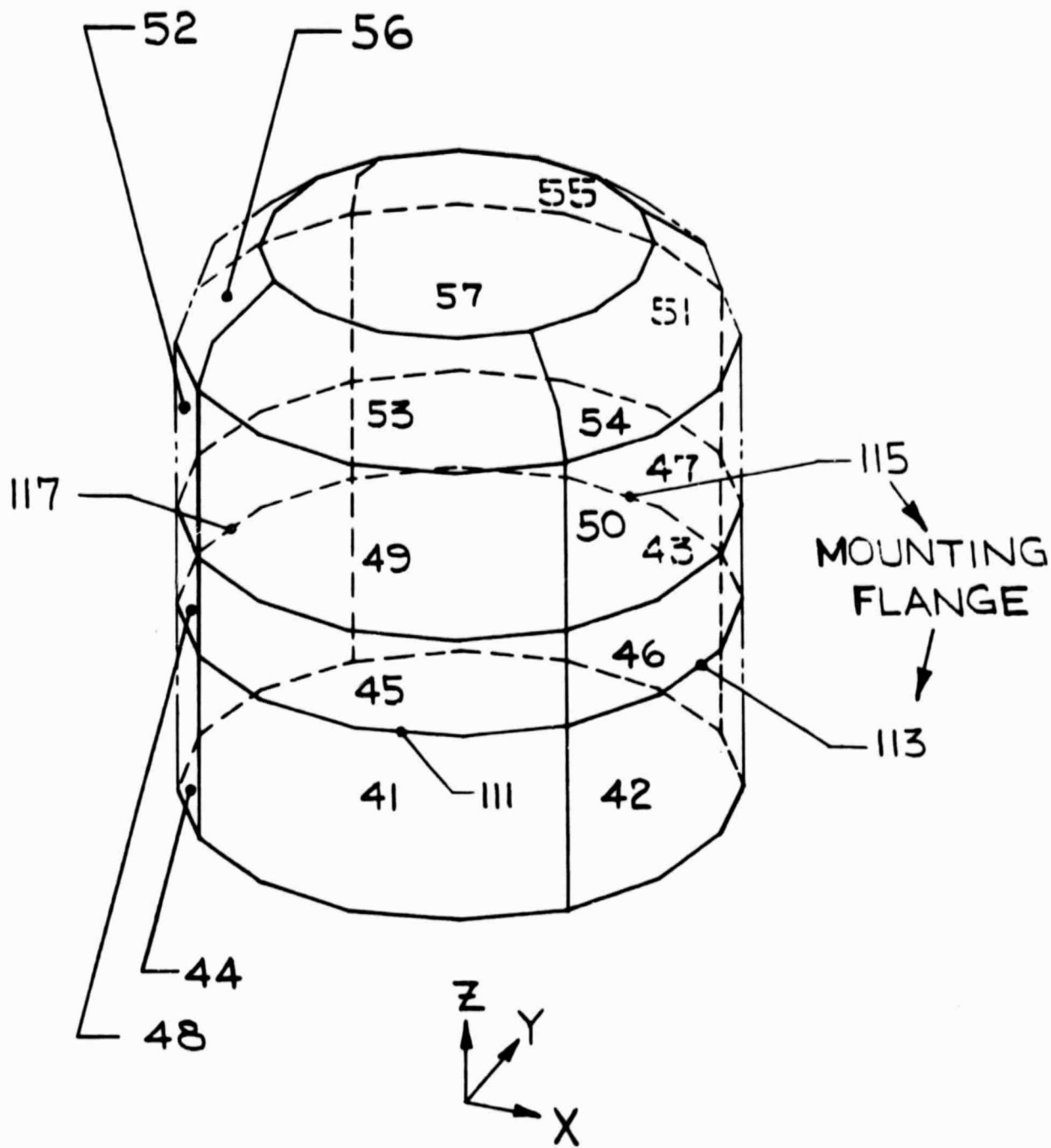


FIGURE 4a. NODE BAEDEKER FOR PRESSURE VESSEL

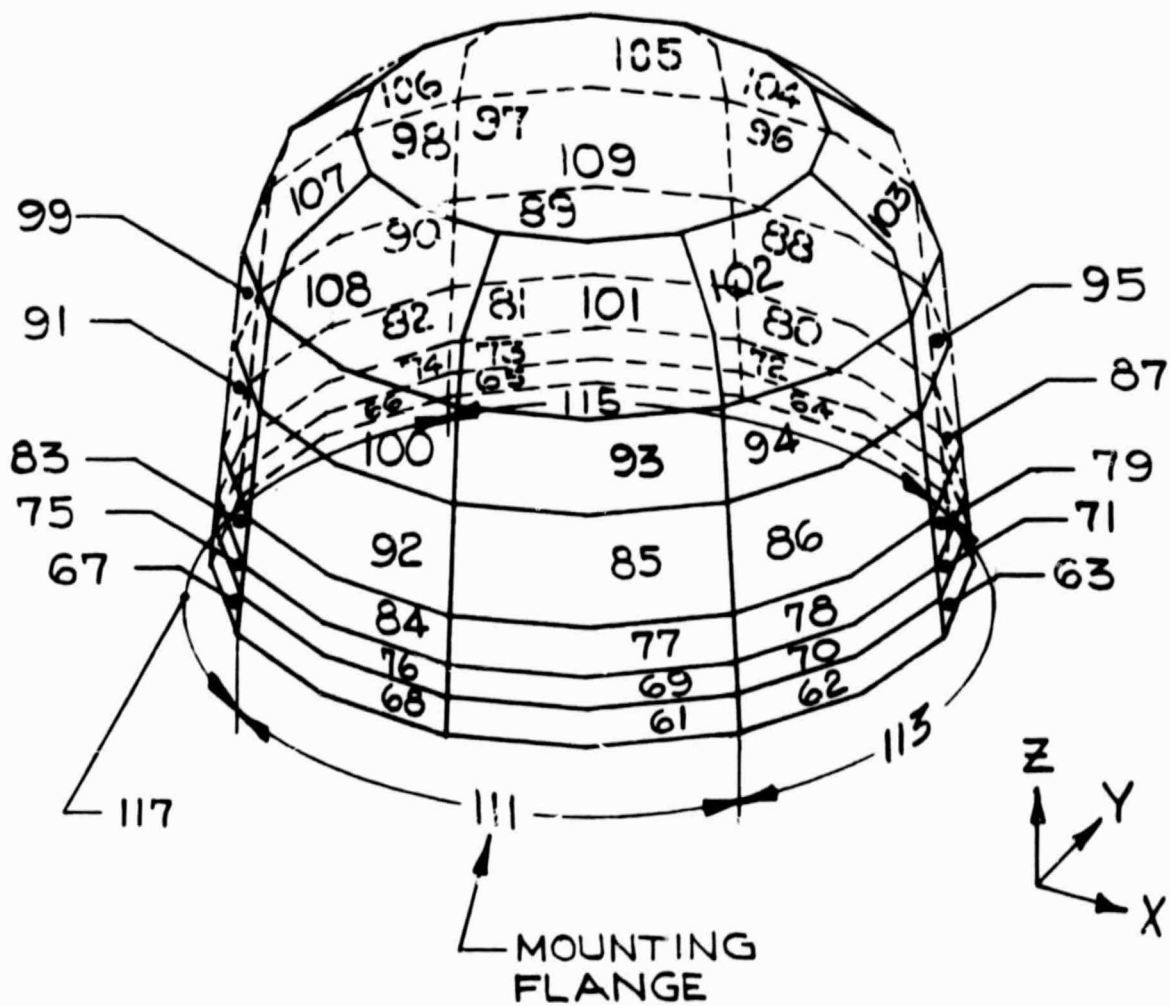


FIGURE 5a. NODE BAEDEKER FOR POLYVINYL TOLUENE DOME



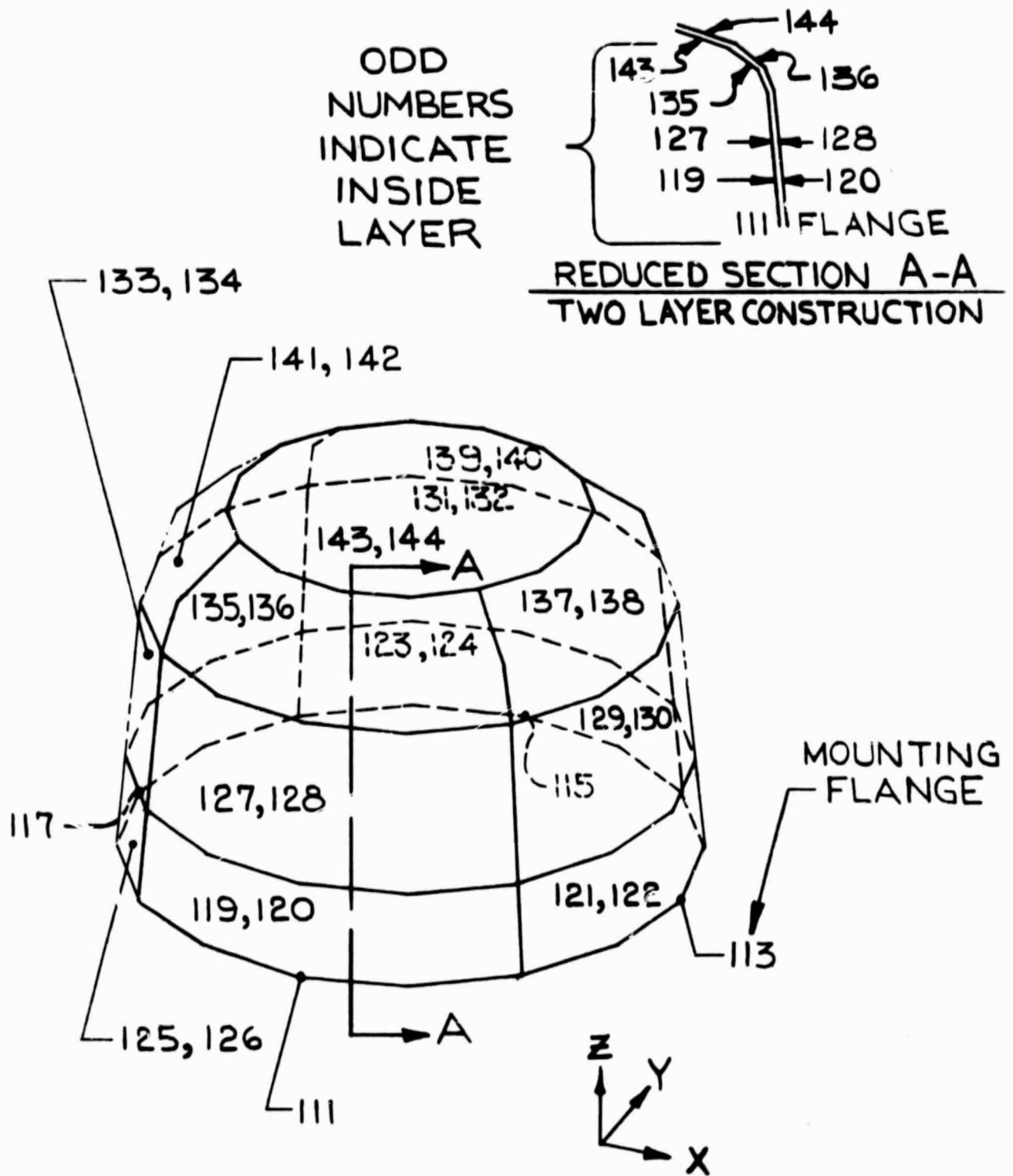


FIGURE 6a. NODE BAEDEKER FOR  
LIGHT SHIELD

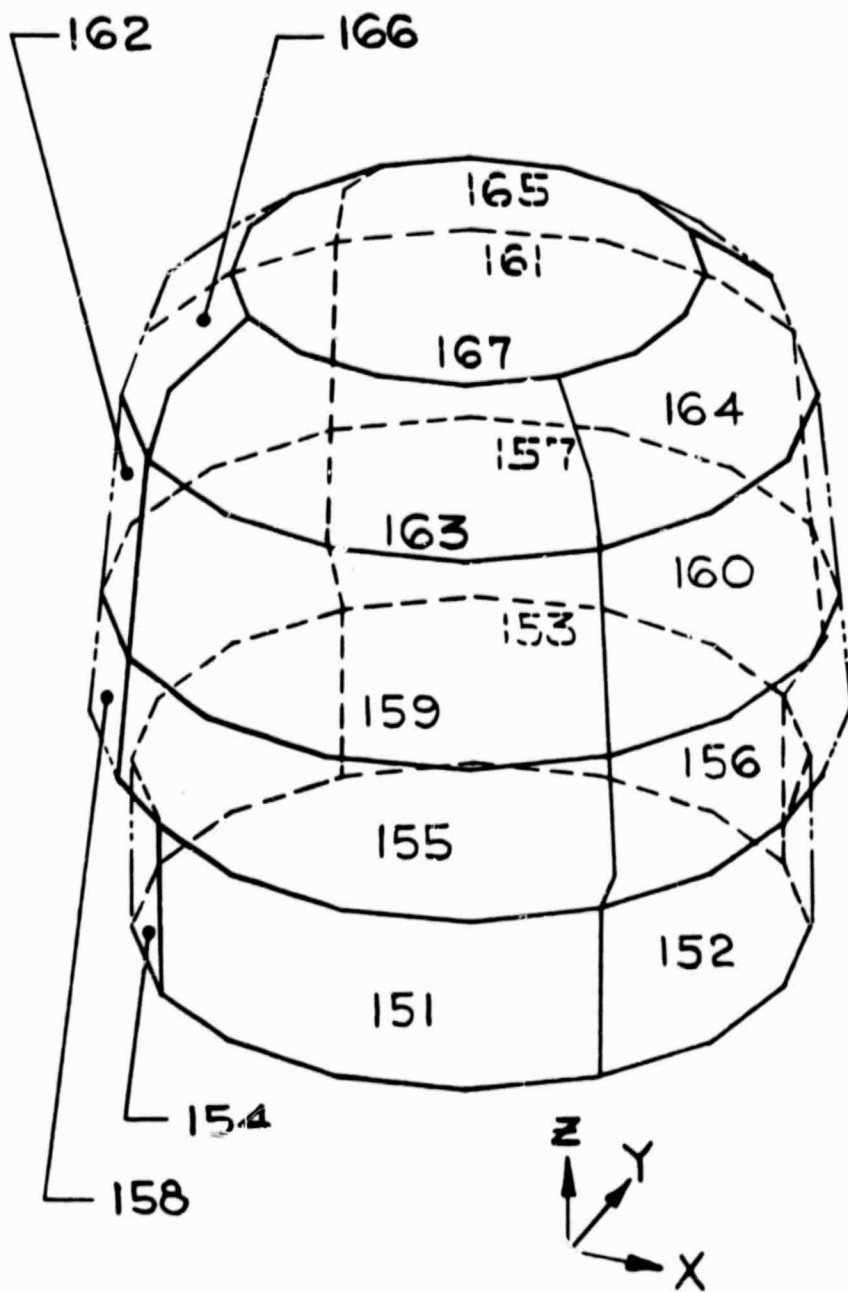


FIGURE 7a. NODE BAEDEKER FOR EXTERIOR LAYER OF MLI THERMAL COVER

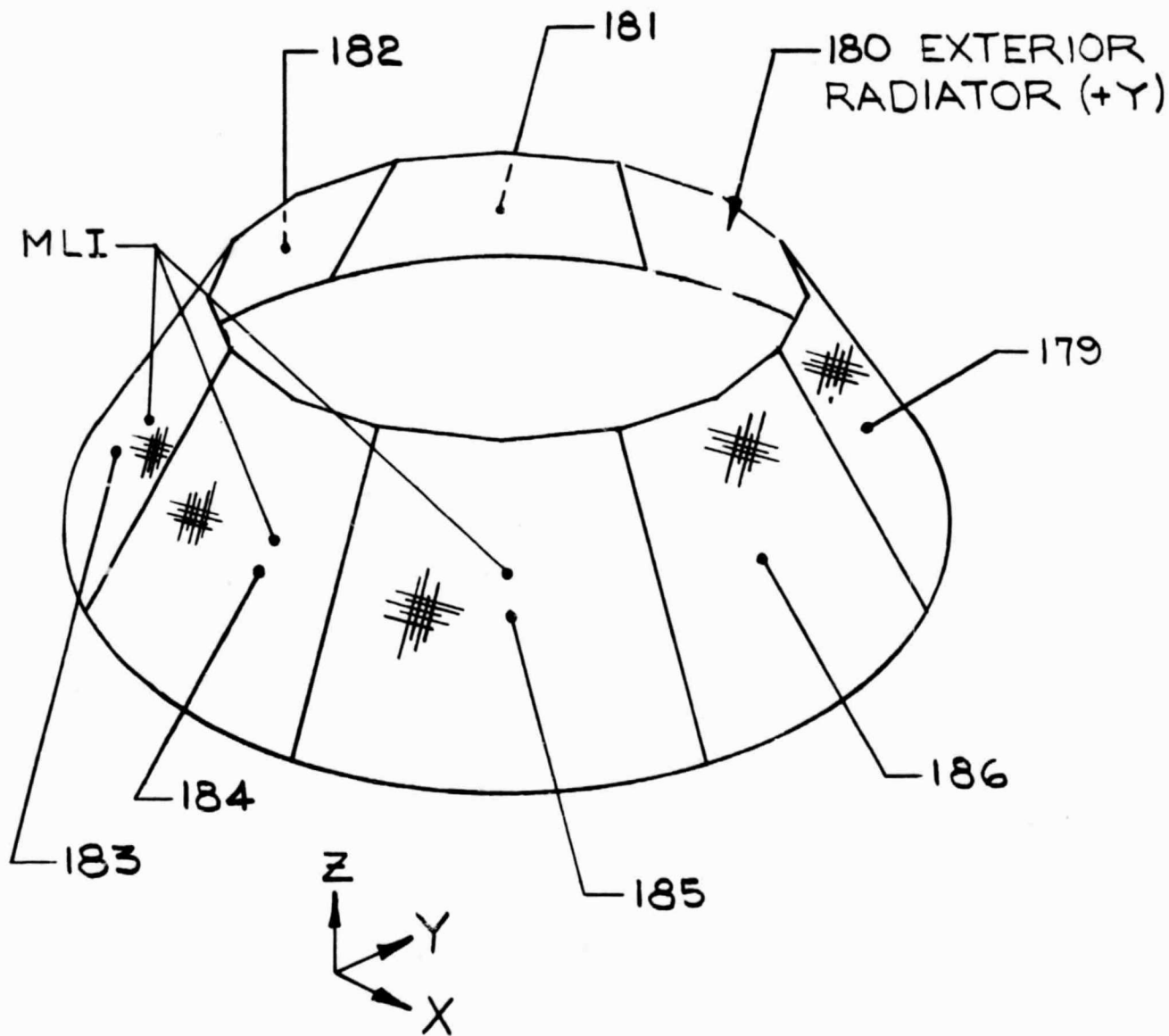


FIGURE 8a NODE BAEDEKER FOR MONOCOQUE SUPPORT STRUCTURE

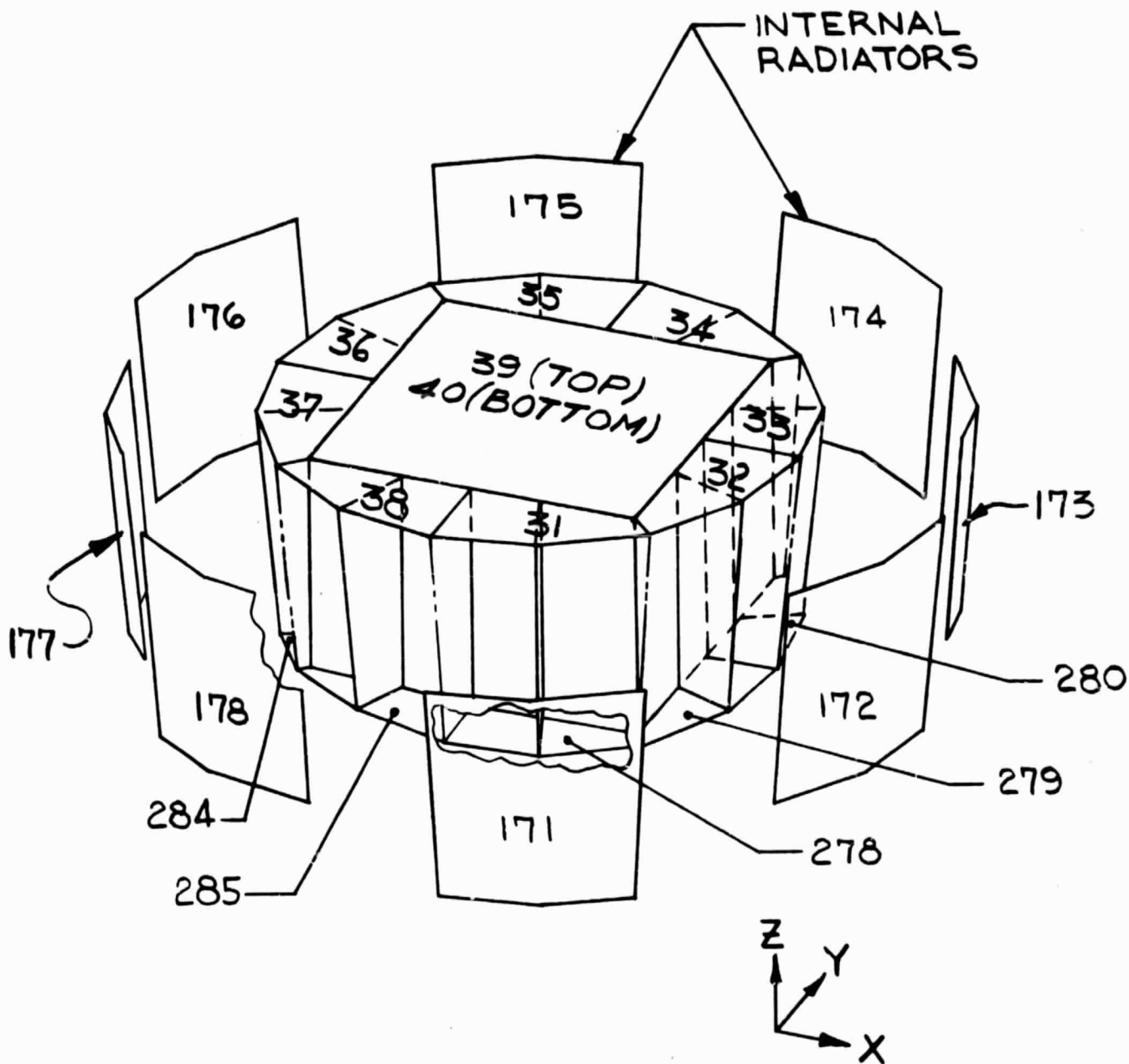


FIGURE 9a NODE BAEDEKER FOR ELECTRONICS COMPARTMENTS

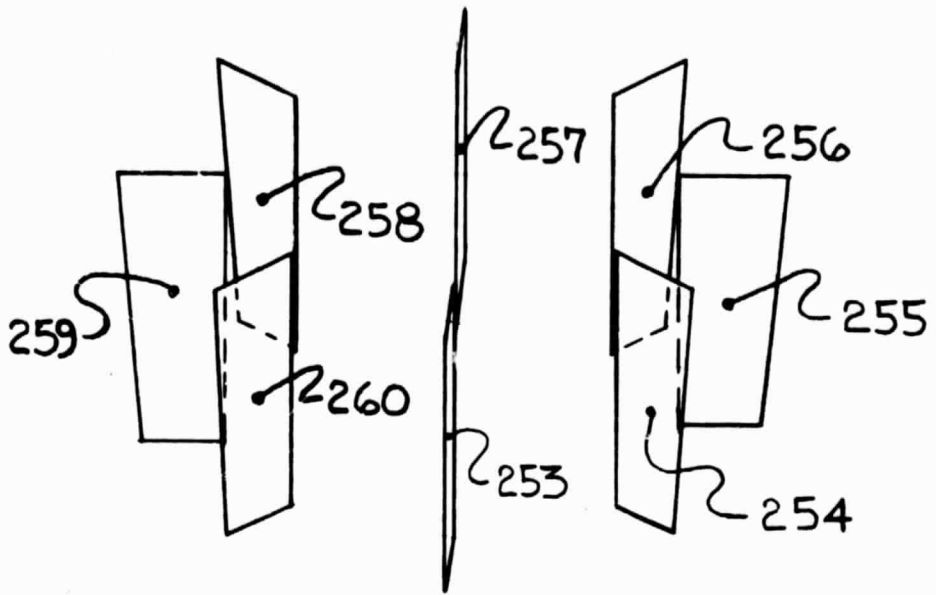


FIGURE 10a NODE BAEDEKER FOR  
VERTICAL SUPPORTS IN  
ELECTRONICS COMPARTMENTS

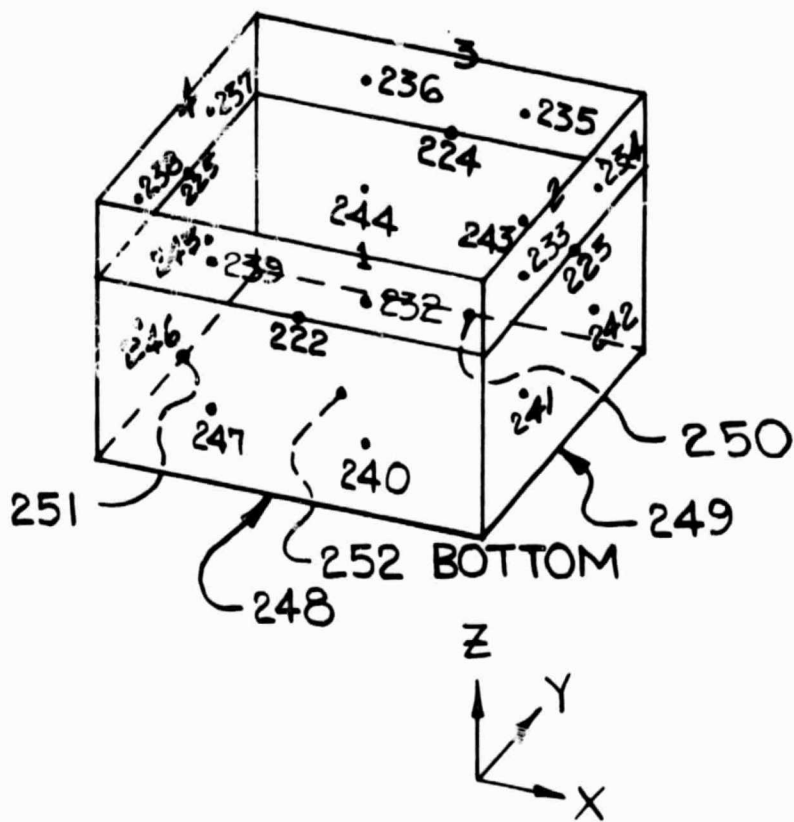


FIGURE 11a NODE BAEDER FOR DEEP  
"I" BEAM CHANNELS ENCLOSING  
TOTAL ADSORPTION SHOWER COUNTER

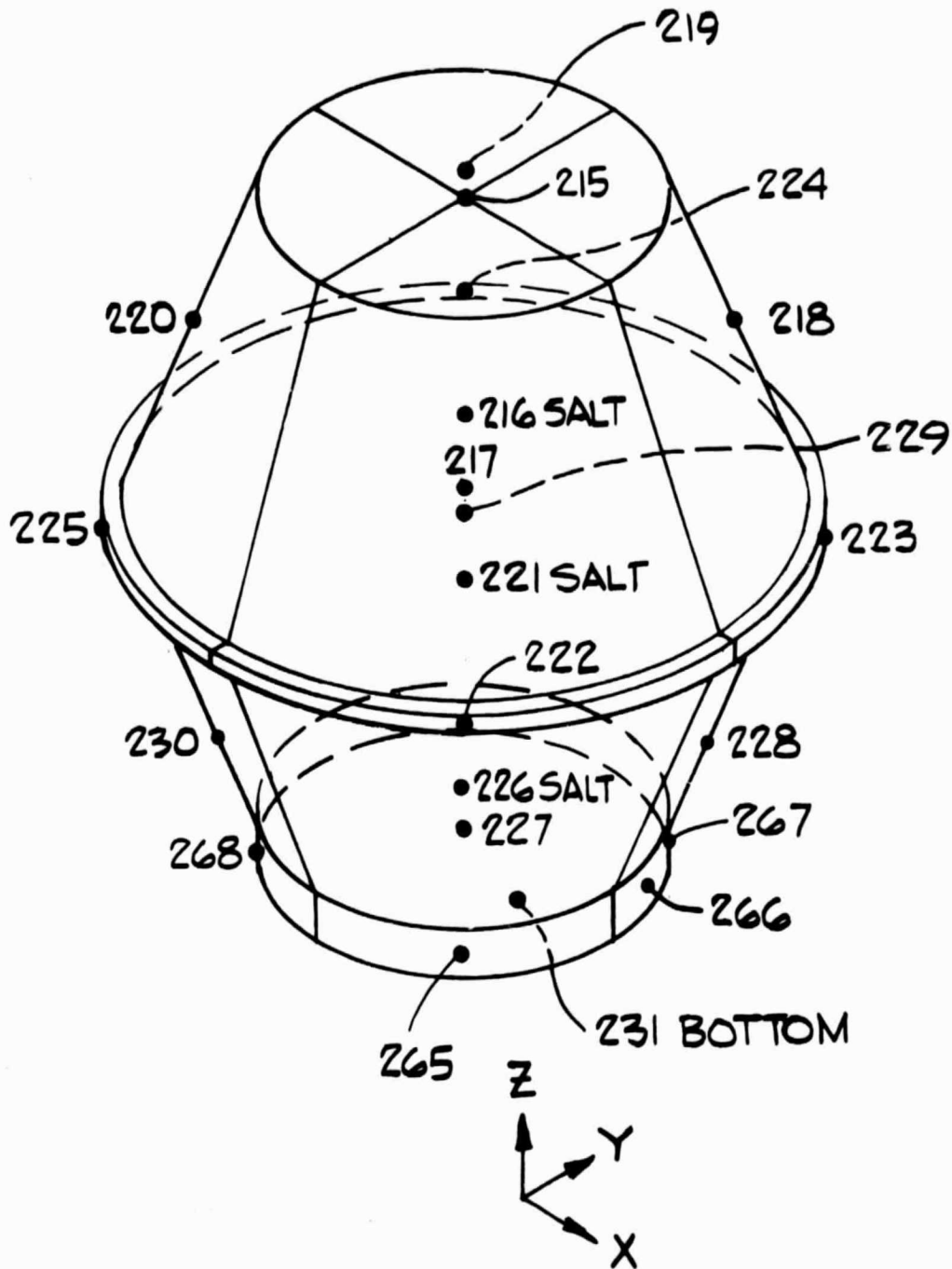


FIGURE 12a NODE BAEDEKER FOR TOTAL ABSORPTION SHOWER COUNTER (TASC)

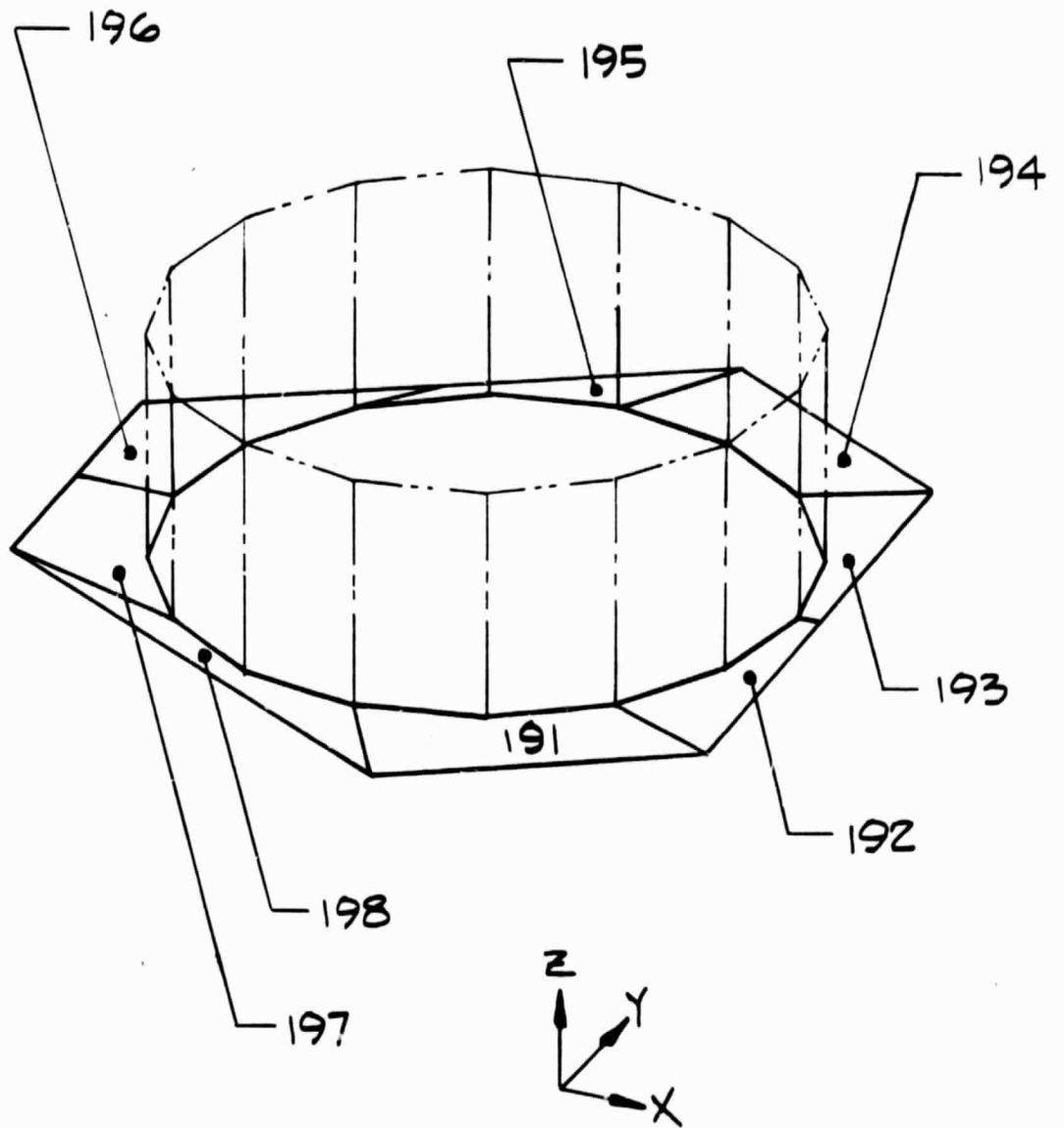


FIGURE 13 a NODE BAEDEKER FOR EXTERIOR LAYER OF MLI ON SPACECRAFT



**APPENDIX B**

**NUMERICAL SURFACE NAMES FOR GEOMETRIC REPRESENTATION OF EGRET**

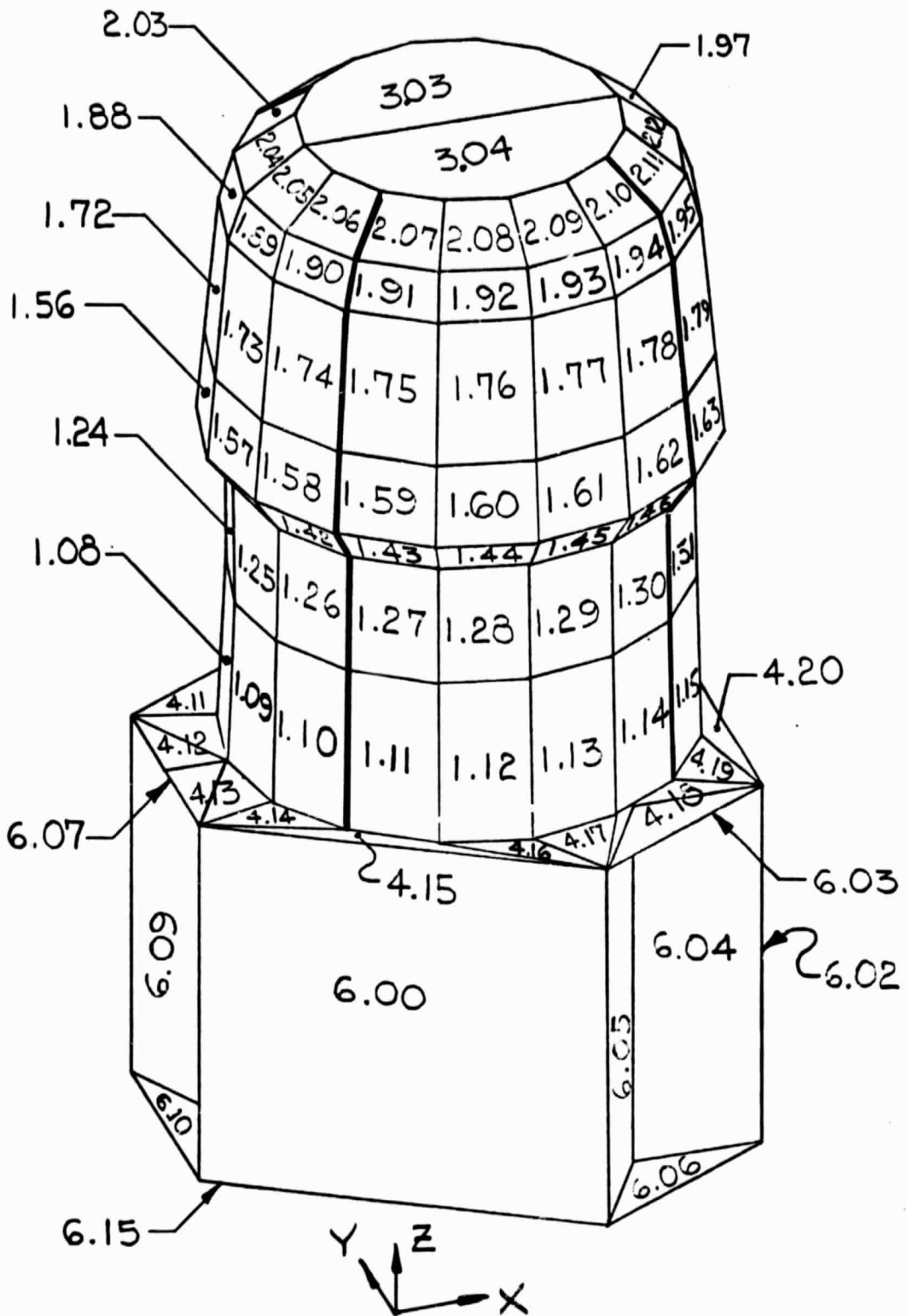


FIGURE 1b SURFACE NOMENCLATURE FOR EXTERIOR GEOMETRIC MODEL OF EGRET

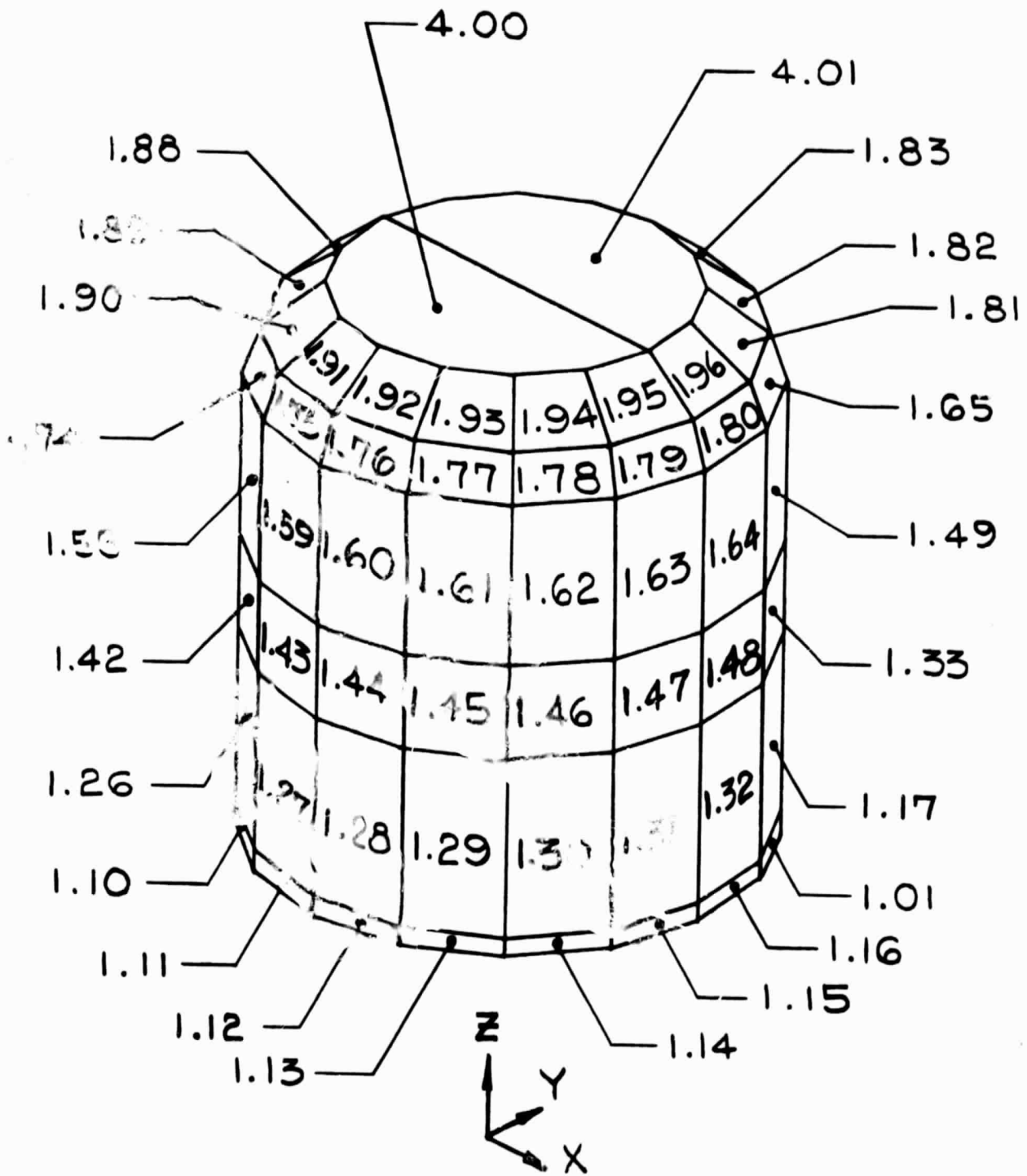


FIGURE 2b SURFACE NOMENCLATURE FOR INTERIOR GEOMETRIC MODEL OF PRESSURE VESSEL

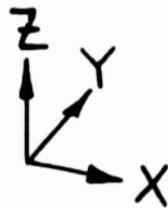
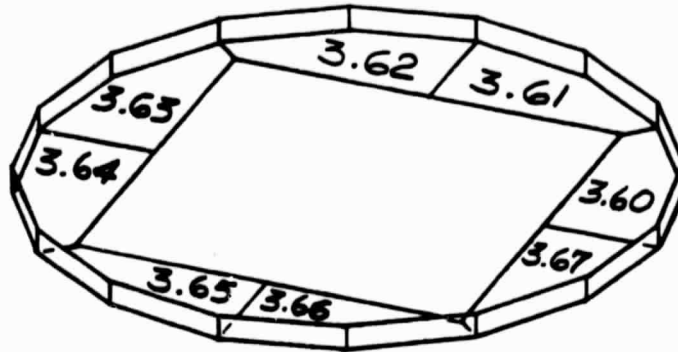


FIGURE 3B SURFACE NOMENCLATURE FOR INTERIOR  
GEOMETRIC MODEL OF PRESSURE  
BULKHEAD

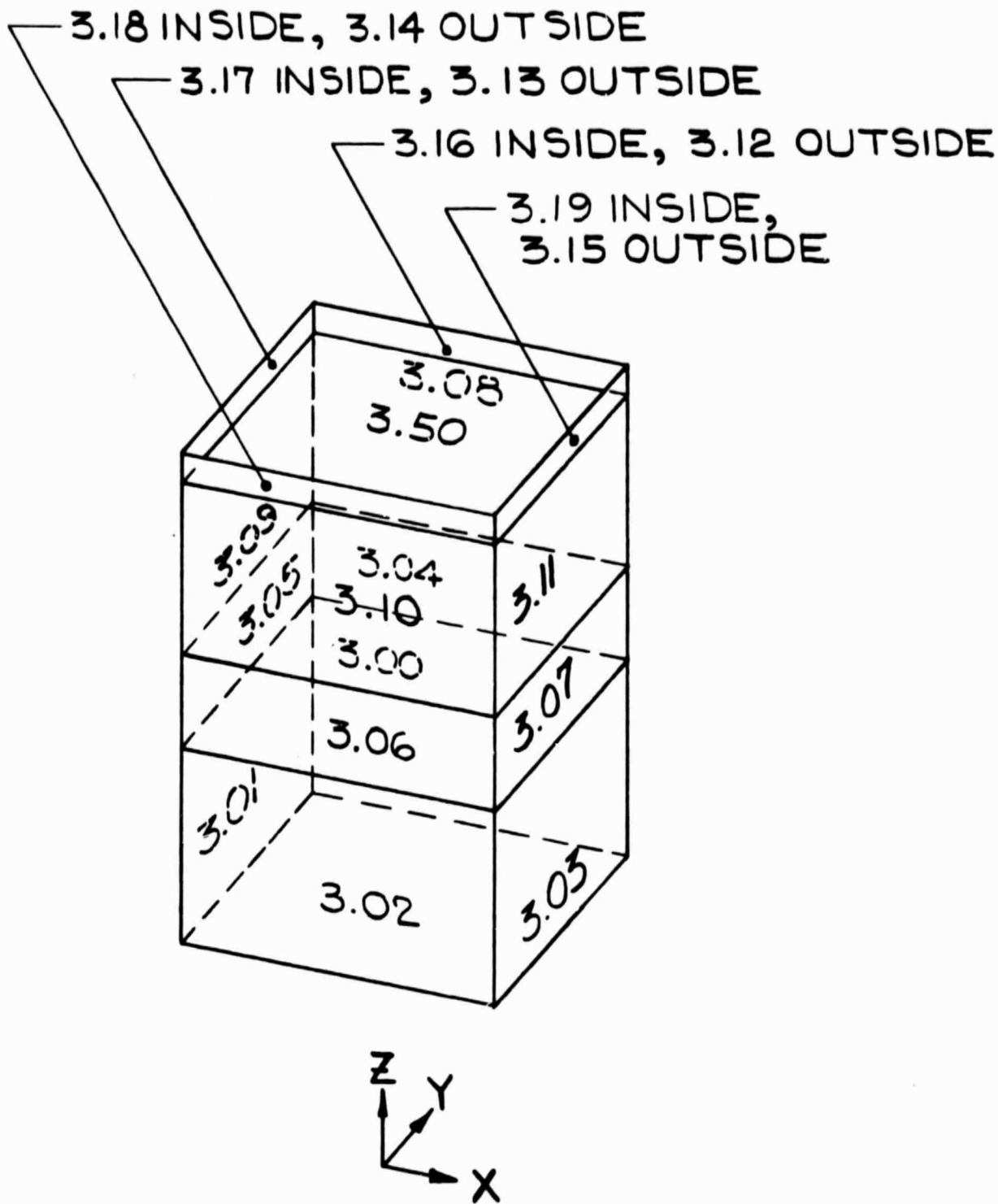


FIGURE 4b SURFACE NOMENCLATURE FOR EXTERIOR GEOMETRIC MODEL OF HIGH VOLTAGE STACK

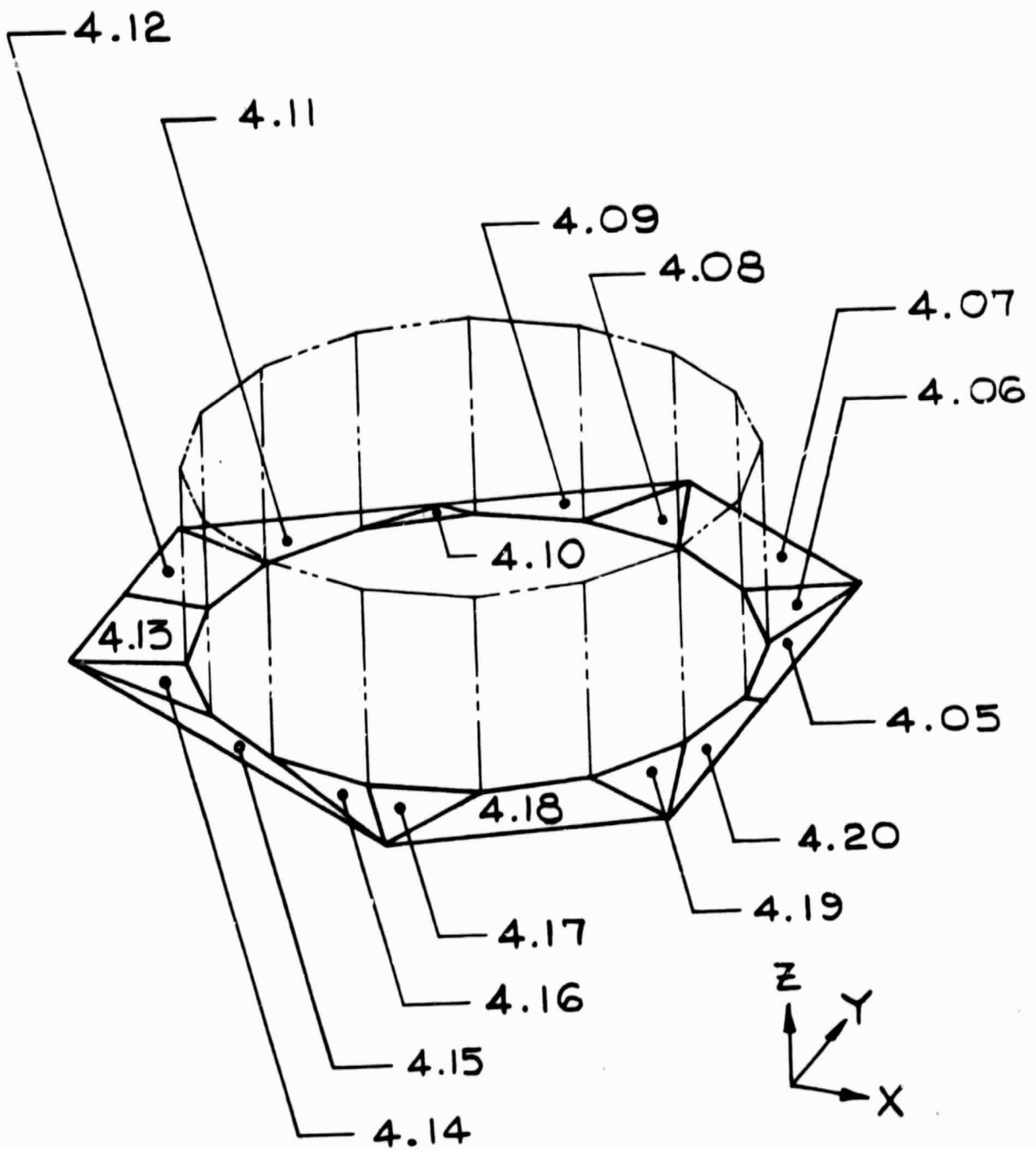


FIGURE 5b SURFACE NOMENCLATURE FOR EXTERIOR LAYER OF MLI ON SPACECRAFT

**APPENDIX C**

**DYNATECH REPORT ON THE THERMAL CONDUCTIVITY OF A PVT PLASTIC**



DYNATECH

Report on

THE THERMAL CONDUCTIVITY  
OF A PVT PLASTIC

For: Arthur D. Little, Inc.  
20 Acorn Park  
Cambridge, Massachusetts 02140

A specimen of a clear plastic described as PVT was submitted for the analysis of thermal conductivity. The specimen was 18.8 mm diameter x 1.26 mm thick having a density of  $1035 \text{ kgm}^{-3}$ .

Experimental Procedure

The thermal conductivity was determined using the Colora Thermoconductometer. The sample was placed between ground silver plates which could be kept at the given boiling points of two liquids by a constant supply of heat to the higher boiling point liquid. When steady equilibrium was attained, the lower boiling point liquid vaporized at a constant rate and was condensed and collected in a measuring vessel. The time for a given volume to distill was measured.

The thermal conductivity was calculated from

$$\lambda = (q/\Delta T) (x/A)$$

where  $q/\Delta T$  = reciprocal thermal resistivity obtained from calibration curves  
 $x$  = specimen thickness  
 $A$  = specimen cross sectional area

The results are shown in the following table

TABLE  
THE THERMAL CONDUCTIVITY OF A  
SPECIMEN OF PVT PLASTIC

<u>Temperature, C</u>	<u>Thermal Conductivity, <math>\text{Wm}^{-1}\text{degK}^{-1}</math></u>
40	0.18
93	0.17 (Sample softened)

*Progress through Research*